Prepared for:

Utah Division of Air Quality
Science for Solutions Research Grant – FY 2020
Salt Lake City, UT

Prepared by:

Chris Emery, Dr. Marcus Trail, Dr. Chris Lindhjem, Tejas Shah, Yesica Alvarez,
Sai Sreedhar Varada, Dr. Greg Yarwood
Ramboll US Corporation
50 West Broadway, Suite 300
Salt Lake City, UT

May 2020
1690014052

Investigating Sources of Ammonia Uncertainty in Modeling the Salt Lake City $PM_{2.5}$ Nonattainment Area

Photo by Aaron Gustafson (CC BY-SA)

RAMBOLL Bright ideas. Sustainable change.

Investigating Sources of Ammonia Uncertainty in Modeling the Salt Lake City $PM_{2.5}$ Nonattainment Area

Acknowledgements:

This project was primarily funded by a State of Utah FY20 Science for Solutions research grant, through the Utah Department of Environmental Quality, contract number 200046. We thank the Utah Division of Air Quality staff for contributions to the project, including the modeling datasets, technical assistance and information, and review of this report.

We thank Marathon Petroleum for co-funding this study.

We thank Dr. Randy Martin, Utah State University, for providing information about the Winter 2019 Wasatch Front Ammonia and Chloride Observations (WaFACO) field study.

Ramboll
7250 Redwood Boulevard
Suite 105
Novato, CA 94945
USA

T +1 415 899 0700
https://ramboll.com

CONTENTS

Table of Figures

Table of Tables

Acronyms and Abbreviations

µg	microgram
°F	Degrees Fahrenheit
°C	Degrees Centigrade or Celsius
AMOX	Ammonia oxidation
BTS	Bureau of Transportation Statistics
C	Compensation point for surface re-emission
CAMx	Comprehensive Air quality Model with extensions
CB6r2h	Carbon Bond 6 photochemical mechanism, release 2 with halogen chemistry
CH_4	Methane
Cl	Chorine/chloride
$ClNO_2$	Nitryl chloride
CNG	Compressed natural gas
CO	Carbon monoxide
CO_2	Carbon dioxide
DV	Design value
E85	"Flex Fuel" gasoline comprising 85% ethanol by volume (variations allowed in US)
EC	Elemental carbon
EPA	US Environmental Protection Agency
EQSAM	Inorganic equilibrium particulate chemistry module
FCRS	Fine primary inorganic crustal particulate matter

FPRM	Fine primary inorganic particulate matter
FRM	Federal Reference Method
ft	feet
FTP	Federal Test Procedure
g	gram
H_2	Hydrogen
H_2O	Water
HCl	Hydrochloric acid
hp	horsepower
HPDI	High-pressure direct injection
hr	hour
ISORROPIA	Inorganic equilibrium particulate chemistry module
kg	kilogram
km	kilometer
kW	kilowatt
m	meter
m^3	cubic meter
mg	milligram
MOVES	Motor Vehicle Emission Simulator
MP	Maintenance plan
N_2O_5	Dinitrogen pentoxide
N_2O	Nitrous oxide
Na	Sodium
NAA	Nonattainment area
NAAQS	National Ambient Air Quality Standard
NEDC	New European Driving Cycle
NH_3	Ammonia (gas)
NH_4	Ammonium (particulate)
NHTSA	National Highway Traffic Safety Administration
NMB	Normalized mean bias
NME	Normalized mean error (unsigned or gross error)
NO	Nitric oxide
NO_2	Nitrogen dioxide
NO_3	Nitrate
NOx	Nitrogen oxides ($NO + NO_2$)
O_3	Ozone
OC	Organic carbon
OA	Organic aerosol
Ox	Odd oxygen ($Ox = NO_2 + O_3$)
PCAP	Persistent cold air pool
PEMS	Portable Emission Monitoring System
$PM_{2.5}$	Particulate matter with aerodynamic diameter less than 2.5 microns
ppb	part per billion
ppm	part per million
R	Resistance to surface deposition
RADM	Regional Acid Deposition Model aqueous inorganic particulate chemistry module
RWC	Residential wood combustion
SCR	Selective Catalytic Reduction
SIP	State implementation plan

SLC	Salt Lake City
SMAT	Speciated Modeled Attainment Test program
SMOKE	Sparse Matrix Operator Kernel Emissions processor
SO_2	Sulfur dioxide
SO_4	Sulfate
SOA	Secondary organic aerosol
SOAP	Secondary Organic Aerosol chemistry module
TPD	Tons per day
TSD	Technical support document
TWC	Three-way catalyst
UC	Unified Cycle
UDAQ	Utah Division of Air Quality
UDDS	Urban Dynamometer Driving Schedule
ULEV	Ultra-Low Emissions Vehicle
USU	Utah State University
UWFPS	Utah Winter Fine Particulate Study
VOC	Volatile organic compound
WaFACO	Wasatch Front Ammonia and Chloride Observations Study
WLTC	Worldwide Harmonized Light Vehicles Test Cycle
WRF	Weather Research and Forecasting model

1.0 EXECUTIVE SUMMARY

During periodic winter stagnation episodes along the Wasatch Front, 24-hour fine particulate ($PM_{2.5}$) concentrations can exceed the US National Ambient Air Quality Standard (NAAQS), primarily due to a buildup of ammonium nitrate. Over the past several years, the Utah Division of Air Quality (UDAQ) has developed a photochemical modeling application to support the State Implementation Plan (SIP) and subsequent Maintenance Plan (MP) for the Salt Lake City (SLC) 24-hour $PM_{2.5}$ Serious Nonattainment Area. During SIP development, UDAQ found that the model substantially under predicted ammonium nitrate primarily because of a lack of ammonia (NH_3) but had little information on likely causes for the NH_3 shortfall, whether by inventory inaccuracies and/or model deficiencies. UDAQ addressed the shortfall by adding additional NH_3 emissions based on model-measurement differences by county, and then holding that additional quantity constant into the future year model projections. The need to supply the model with additional NH_3 emissions from unknown sources presents a major model uncertainty that may affect the accuracy of projected future $PM_{2.5}$ levels. This project investigated causes for the apparent NH_3 shortfall and benefitted from the Wasatch Front Ammonia and Chloride Observations (WaFACO) field study conducted by Utah State University (USU) during the winter of 2019. We reviewed NH_3 emission inventories and recently measured concentration patterns; investigated modeling uncertainties and deficiencies, updated the UDAQ model configuration and increased modeled NH_3 emissions from on-road vehicles according to peer-reviewed literature; and re-evaluated modeling results and projected attainment-year $PM_{2.5}$ air quality.

Based on comparisons to routine field measurements during the January 1-10, 2011 modeling episode, the UDAQ simulation replicated the relative contributions of most $PM_{2.5}$ species rather well but under predicted total $PM_{2.5}$ at all sites throughout the episode because of a lack of particulate ammonium nitrate, despite the additional NH_3 emissions. The simulated meteorology generally captured the build-up and cessation of the stagnant inversion pattern over the episode. However, comparison of observed and predicted concentrations of carbon monoxide and nitrogen oxides (NOx), which depend on different emission inventory sectors than ammonia, indicated that simulated meteorology did not sufficiently characterize inversion strength/depth, dispersion patterns or the degree of stagnation in time and space. We found that on average NOx was under predicted by about 20% during the episode while ozone was consistently over predicted. During mid-episode when $PM_{2.5}$ peaked, modeled chemical relationships among NOx and ozone pointed to low rates of NOx oxidation and the lack of nitrate production. Additionally, we found that even with UDAQ's additional NH_3, simulated NH_3 concentrations over the basin remained roughly a third of the average 11-12 ppb measured in SLC during the February 2019 WaFACO study.

On the basis of model sensitivity testing, we found that simulated $PM_{2.5}$ and most gas concentrations benefitted from reduced vertical mixing, which also reduced the apparent NH_3 shortfall, and likewise benefited from increased snow albedo, which enhances photochemical production of secondary species including nitrate. However, the model was insensitive to the introduction of bi-directional NH_3 surface exchange because the presence of snow cover squelches NH_3 re-emission from soil/vegetation. Additionally, snow enhances NH_3 deposition rates when snow partially melts during the daytime. The model was also insensitive to chemical modifications such as invoking alternative inorganic aerosol chemistry, removal of clouds (maximized solar radiation), increased chloride levels (increased oxidant production), and a scale-up of NOx emissions to alleviate the episode-average NOx under prediction bias.

Simulated NH_3 and ammonium nitrate concentrations responded most favorably when we replaced the UDAQ NH_3 injection with a scale-up of on-road vehicle NH_3 emissions by a factor of ~2, a modification

that is supported by the scientific literature. While the UDAQ NH_3 injection added ~65% to the original total Salt Lake County episodic emission inventory, the on-road NH_3 scale-up added ~40%. Although we found major uncertainties in other NH_3 emission sectors, specifically animal husbandry and landfill/composting facilities, we did not alter those NH_3 emissions because of a lack of information needed to address fundamental issues with emission factors (emission rates per activity unit), a lack in estimated activity (animal head counts, composting volumes) and the manner in which these sources are spatially allocated to the modeling grid (to general landuse categories rather than to specific locations/facilities). In the more rural counties of Box Elder, Weber, Tooele, and Utah under estimates of agricultural NH_3 are likely to be the primary cause for $PM_{2.5}$ under predictions.

We conducted a final 2011 base-year simulation for the episode, applying reduced vertical diffusion rates, increased urban snow albedo, and scaled-up on-road vehicle NH_3 emissions in lieu of the UDAQ NH_3 injection. While the model continued to under predict total $PM_{2.5}$, particularly at rural monitoring sites, agreement with speciated $PM_{2.5}$ measurements improved markedly at the urban monitoring sites relative to UDAQ's simulation. The final model configuration predicted particulate sulfate well and approached the 2019 episode-averaged measured concentrations of NH_3 in the Salt Lake basin. However, the model continued to under estimate particulate nitrate by 35%, similarly to UDAQ's results, over all speciated monitoring sites and monitored days. This performance is consistent with and generally better than other $PM_{2.5}$ modeling applications in the western US. This case also revealed that carbon emissions from sources such as smoke may be over estimated in the SLC area and that the split among primary organic and elemental carbon emissions may need adjustment at the source-category level.

Finally, we conducted simulations using UDAQ's 2017 and 2019 projected emission inventories, applying the on-road vehicle NH_3 scale-up at the same proportion as 2011, and holding the model configuration and all other model inputs the same as the final base-year simulation described above. Results among UDAQ and Ramboll projected $PM_{2.5}$ design values (DV) from 2016-2018 monitored DVs were very similar with no sites projected to exceed the NAAQS. We confirmed that both our and UDAQ's projected cases do result in some small concentration increases for inorganic secondary salts (ammonium, nitrate and sulfate), indicating disbenefit conditions.

Both modeled and measured ozone and NOx indicate that the gas-phase chemical environment that generates secondary $PM_{2.5}$ compounds during exceedance events is NOx-saturated and oxidant-lean. This is a separate issue from whether $PM_{2.5}$ formation is ammonia- vs. nitrate-limited. In a NOx-saturated environment, NOx emission reductions can raise oxidant levels, raise secondary PM formation rates, and cause $PM_{2.5}$ increases or smaller-than-expected decreases ("NOx dis-benefit"). Recent field studies and previous UDAQ analyses indicate the SLC atmosphere is typically in a NOx-saturated regime during stagnant inversions and the model behaves consistently with this pattern. This has major implications for accurately projecting future $PM_{2.5}$ based on anticipated emission inventory changes. Additionally, our results provide ample evidence to suggest that the inorganic $PM_{2.5}$ environment in SLC can vary spatially and temporally between NH_3-limited and nitrate-limited conditions. The model is therefore responding appropriately to emission reductions with small reductions or increases in $PM_{2.5}$, although its degree of response is affected by uncertainties and could change substantially if the particulate nitrate bias was corrected. Remaining model performance issues are related to the ability of the meteorological model to properly represent weak flow patterns under stagnant inversion conditions, and remaining issues for certain stationary emission sectors, including activity, spatial distribution, temporal allocation, and speciation including the split of primary $PM_{2.5}$ emissions into specific carbon and non-carbon components.

Based on results from this study, we recommend the following for future research and modeling applications:

- Continue to employ the updates developed in this project for future $PM_{2.5}$ modeling analyses, including reduced vertical diffusion rates, increased on-road vehicle NH_3 emissions, and increased snow-covered urban albedo;
- Bring the modeling system forward to a more recent exceedance episode to characterize contemporary $PM_{2.5}$ air quality along the Wasatch Front and to update future year projections;
- Investigate ways to improve the meteorological simulation of persistent cold air pool (PCAP) episodes along the Wasatch Front, specifically in characterizing inversion depth and strength, three-dimensional dispersion patterns, and boundary layer cloud evolution;
- Improve NH_3 emission inventory and spatial allocation techniques for remaining key sources: livestock agriculture (particularly in more rural counties) and landfill/composting activities;
- Investigate causes for under estimates of NOx and chloride emissions;
- Research and implement alternative speciation profiles for wood combustion among organic and elemental carbon and non-carbon smoke components;
- Investigate how the collection of further model updates alter $PM_{2.5}$ response to future projected and/or alternative emissions scenarios;
- Further investigate the role of snow in modulating surface-atmosphere NH_3 exchange;

2.0 INTRODUCTION

2.1 Background

Salt Lake City (SLC) and Utah County are designated as Serious Nonattainment Areas (NAA) for the 2006 24-hour fine particulate ($PM_{2.5}$) National Ambient Air Quality Standard (NAAQS). To support the State Implementation Plan (SIP) revision for SLC, the Utah Division of Air Quality (UDAQ) demonstrated attainment of the $PM_{2.5}$ standard by the attainment year of 2019 based on photochemical modeling and weight-of-evidence analyses (UDAQ, 2018). On October 28, 2019, the US Environmental Protection Agency (EPA) finalized a clean data determination for SLC based on monitoring data for the period 2016-2018 (EPA, 2019a). However, this determination itself does not re-designate the area to attainment, and any future $PM_{2.5}$ NAAQS violations will trigger requirements for revised attainment plans. UDAQ has since developed a Maintenance Plan (MP) for SLC that includes future projections of $PM_{2.5}$ air quality out to 2035 based on the SIP photochemical modeling application (UDAQ, 2020a).

According to the MP, related Technical Support Documents (TSD), and the 2017 Utah Winter Fine Particulate Study (UWFPS; Baasandorj et al., 2018), $PM_{2.5}$ concentrations can exceed the standard during wintertime persistent cold air pool (PCAP) events. Over 70% of exceedance-level $PM_{2.5}$ mass is comprised of compounds that are chemically formed in the atmosphere from direct emissions of gas precursors. The dominant $PM_{2.5}$ component is ammonium nitrate, formed from ammonia (NH_3) emissions and the photochemical processing of nitrogen oxide (NOx) emissions. UDAQ's photochemical modeling of a historical PCAP event in January 2011 replicated measured $PM_{2.5}$ concentrations and composition adequately well, but only after artificially increasing NH_3 emissions by 200% over the six Wasatch Front counties comprising SLC and Utah NAAs to make up for an apparent lack of inventoried NH_3. UDAQ made clear that the artificial NH_3 addition is a major model uncertainty that may affect the accuracy of the modeled attainment projections because it impacts the ability to predict how $PM_{2.5}$ differentially responds to projected changes in NH_3 and NOx emissions. During model development, there was little information on whether the NH_3 shortfall was caused by inventory inaccuracies or model deficiencies. However, peer-reviewed literature (Sun et al., 2014) indicates that the MOVES[1] motor vehicle emission factor model (EPA, 2019b) used by UDAQ under predicts NH_3 emissions. Additionally, the photochemical model employed by UDAQ lacks a "bidirectional" surface NH_3 exchange mechanism, a potentially important mechanism by which NH_3 deposited to the surface can subsequently re-volatilize back to the air.

2.2 Purpose and Objectives

In this project we investigated causes for the modeled NH_3 shortfall and tested model improvements that result in a more robust modeling application. Specific activities included:

1. Review current NH_3 inventories and estimation procedures, and spatial and temporal concentration patterns measured during recent (2017 and 2019) winter PCAP field studies;
2. Quantify NH_3 emission uncertainties for key sources, with particular attention to on-road vehicle emissions;
3. Investigate uncertainties in the modeling system, apply an updated model version that includes bidirectional NH_3 exchange with soil and vegetation, and investigate $PM_{2.5}$ sensitivity to NH_3 and NOx emissions;
4. Refine modeled NH_3 emissions from information developed above and re-evaluate modeled results against measurements; and

[1] MOtor Vehicle Emission Simulator (MOVES)

5. Compare UDAQ's projections of $PM_{2.5}$ for the 2019 attainment year against those from the updated model.

This project benefitted from the Wasatch Front Ammonia and Chloride Observations (WaFACO) field study conducted by Utah State University (USU) during the winter of 2019 (UDAQ, 2020b). The study included weekly-integrated sampling at 40 passive monitors throughout the basin, one real-time monitor placed at two different locations, a mobile van from EPA, and 10 mini-vol filter sites for ionic analysis in targeted areas, with 3-4 co-located sites for elemental and carbon analysis.

2.3 A Brief Primer on $PM_{2.5}$ Sources and Chemistry

We include this brief overview as background information for the technical discussions that follow. $PM_{2.5}$ commonly includes a multitude of primary (directly emitted) and secondary (chemically-formed) inorganic and organic compounds from a large variety of sources. Therefore, photochemical models must address numerous precursor and product chemical species, incorporate complex chemical pathways, and characterize all sources, sinks, and dispersion patterns throughout an airshed to correctly estimate the evolution of $PM_{2.5}$ mass budgets. The components of PM include:

- Primary PM includes dust (from agriculture, mining, construction, windblown, vehicle re-entrainment), inorganic and organic carbon particles from combustion sources (from fires, residential wood combustion, cooking, vehicle exhaust), sodium chloride (NaCl; from oceans and dry lake playas), and other minor components from industrial and commercial activities. Stagnant winds, snow cover and/or wet surfaces limit dust and natural salt emissions during winter PCAP events in the SLC, while cold temperatures amplify primary carbon emissions from residential wood combustion and snow cover may increase emissions from road salting.
- Sulfate (SO_4) is formed from the oxidation of sulfur dioxide (SO_2) emissions via two pathways: homogeneous gas-phase photochemistry and heterogeneous aqueous-phase reactions with hydrogen peroxide and metal catalysts in cloud water. SO_4 always exists as an aerosol, either sulfuric acid or several neutralized forms, depending on available cations such as NH_3. While emissions of SO_2 are relatively minor in SLC, sources include industrial processes and diesel exhaust.
- Nitrate (NO_3) is most commonly formed from the oxidation of NOx emissions via two major pathways: homogeneous gas-phase photochemistry and nighttime hydrolysis of photochemically-derived dinitrogen pentoxide (N_2O_5). NO_3 is volatile, existing either as nitric acid gas or a nitrate aerosol when neutralized by available cations such as NH_3 that have not been preferentially taken up by other acids such as SO_4. NOx is a major constituent of pollution in SLC and derives from every source of combustion such as vehicles, commercial and residential activities, and industry.
- The thermodynamic partitioning among inorganic acids (SO_4, NO_3, hydrochloric acid or HCl) and cations (NH_3, Na and calcium from dust) is highly complex and depends on the relative amounts of each compound and environmental conditions such as temperature and humidity. When NH_3 is in excess relative to NO_3, ammonium nitrate (NH_4NO_3) aerosols can form up to the limit of available NO_3 (a nitrate-limited or sensitive environment); when NO_3 is in excess, the amount of ammonium nitrate depends on available NH_3 (an ammonia-limited or sensitive environment). In either case, the amount of available NH_3 depends on the presence of other acids (SO_4 or HCl).
- Secondary organic aerosols (SOA) are formed from the photochemical processing of aromatic volatile organic compounds (VOC) to intermediate condensable organic gases and subsequent condensation to aerosols depending on volatility, age/oxidation state, and environmental conditions. VOCs are a major constituent of pollution in SLC and derive from combustion and

evaporative sources such as commercial and residential activities, vehicles, and industry. Natural vegetation is another major source of the types of VOCs that generate organic aerosols. However, during winter PCAP episodes, photochemical processing is slow and biogenic emissions are minimal. Therefore, nearly all organic PM in SLC derives from primary emission sources.

The major sinks for $PM_{2.5}$ chemical components and their precursors include dry deposition to the surface and wet deposition by precipitation. Dry deposition refers to the irreversible gravitational settling of PM and the chemical uptake of gases onto surface features such as vegetation, soil, snow, and structures. Wet deposition refers to the uptake of aerosols and gasses into clouds and the scavenging of cloud droplets, ambient aerosols and gases by precipitation. While aerosols and highly soluble gases such as nitric and hydrochloric acids are irreversibly removed by precipitation, other less-soluble gases can release back to the air when the aqueous solution exceeds saturation.

3.0 MODELING DATABASE

The UDAQ photochemical modeling application employs the Comprehensive Air quality Model with extensions (CAMx; Ramboll, 2020), version 6.3. The modeling domain consists of a nested grid system with 1.33 km resolution over the SLC NAA and 4 km resolution over the State of Utah (Figure 3-1). UDAQ applied CAMx to simulate the evolution of pollutant concentrations during a historic PCAP event during January 1-10, 2011. The University of Utah (Crossman and Foster, 2016) developed requisite meteorological inputs for the episode using the Weather Research and Forecasting Model, version 3 (WRF; Skamarock et al., 2008). UDAQ prepared emission inputs for the episode based on triennial 2011 and 2014 statewide inventories and projected the latter to several future years accounting for growth in population and sector-specific activity, on-road vehicle fleet turnover, and current and anticipated emission controls on stationary sources (UDAQ, 2018; 2020). UDAQ processed emissions inventory data to model-ready inputs using the Sparse Matrix Operator Kernel Emissions (SMOKE; CMAS, 2019) processing system, version 3.6.5.

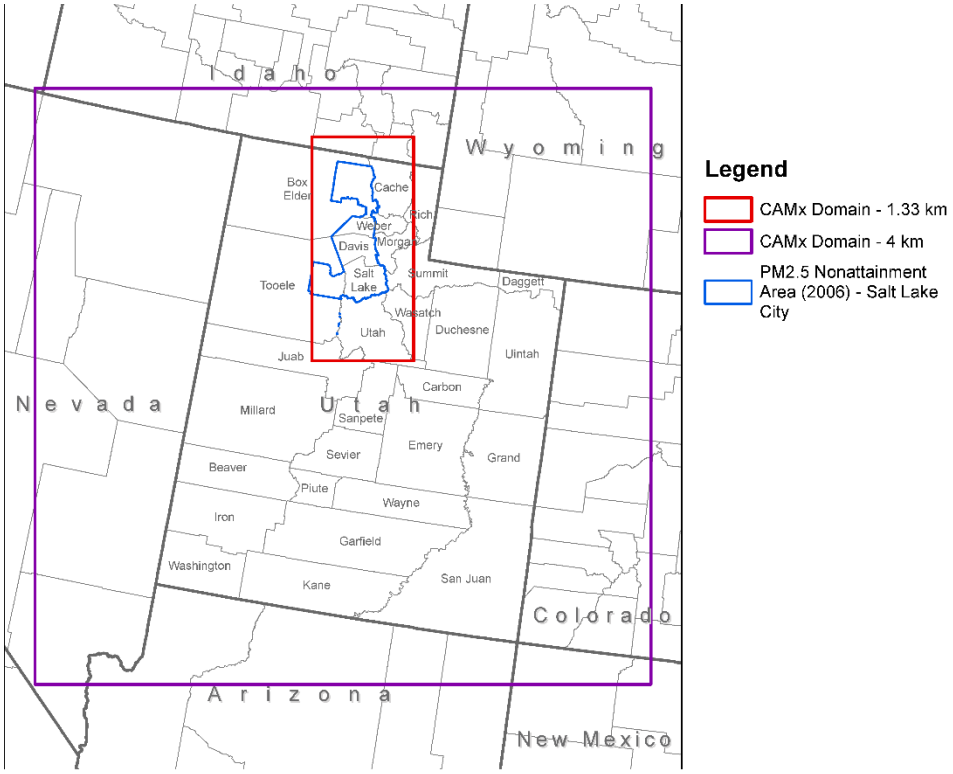

Figure 3-1. The UDAQ nested modeling grids with 4 km grid resolution (outer domain) and 1.33 km grid resolution (inner domain). The SLC NAA is shown for reference.

While developing the modeling system, UDAQ implemented several modifications to improve model performance in replicating the temporal and spatial patterns of measured $PM_{2.5}$ concentrations and composition over the January 2011 episode. Table 3-1 lists the model configuration and modifications implemented by UDAQ; we summarize these below and details are given in the MP (UDAQ, 2020a) and attendant TSDs. One of UDAQ's early modifications involved artificially enhancing the strength and depth of vertical mixing throughout the episode to compensate for over predictions in directly emitted $PM_{2.5}$ components such as road dust. Suspecting that road dust emissions were grossly over estimated, and based on recommendations from EPA, UDAQ later reduced emissions from that sector by 93%. Although this eliminated a key motivation for enhanced vertical mixing, UDAQ preserved

Table 3-1. CAMx v6.3 configuration for the SLC $PM_{2.5}$ modeling system with UDAQ modifications.

CAMx Process	V6.3 Model Configuration	Model/Input Modifications
Advection Solver	Piecewise Parabolic Method	
Gas-Phase Chemistry	Carbon Bond 6 revision 2, with full halogen chemistry (CB6r2h)	
Chemistry Solver	Euler Backward Iterative	
PM Chemistry	2-mode Coarse/Fine, ISORROPIA v1.7 inorganic chemistry (solid+liquid aerosols), RADM aqueous inorganic chemistry, SOAP v1 organic chemistry	
Dry Deposition	Zhang (2001, 2003)	
Wet Deposition	Active	
Vertical Diffusion	Standard K-theory	Increased minimum vertical diffusion rates through 600 m
Surface Albedo		Set minimum urban snow cover fraction = 88%
Dry Deposition		Reduced NH_3 deposition by changing surface resistance from 0 (no resistance) to 1 (full resistance
Dry Deposition		Set ozone deposition to zero
NH_3 Emissions		Injected additional county-level NH_3
Cloud Inputs		Reduced cloud water content of low-altitude clouds over Salt Lake County by 80%

enhanced mixing to the final configuration. One of the most significant modifications involved a large increase in NH_3 emissions by county (by about 65% in Salt Lake County alone) in order to alleviate a large under prediction of ammonium nitrate. The fact that modeled ammonium nitrate concentrations responded so favorably to this change verified that the modeled chemical environment was incorrectly simulating NH_3-limited rather than nitrate-limited conditions as commonly measured in the basin (Baasandorj et al., 2018). But enhanced mixing may have contributed to the large quantity of additional NH_3 needed to reach observed levels. Later, UDAQ reduced the water content of low-altitude clouds over Salt Lake County by 80%, which reduced aqueous sulfate production rates and a related sulfate over prediction bias.

All of the changes described above were made to the emissions and meteorological inputs to CAMx. UDAQ also made the following modifications directly to the CAMx model:

- Setting minimum urban snow cover fraction to 88% as a way to increase net urban surface albedo (solar reflectivity) from the original range of 25-60% to a more representative range of 60-70% (based on albedo measurements of 60-90% during the episode);
- Reducing NH_3 surface deposition rate in order to maintain elevated NH_3 concentrations and further improve model performance for ammonium nitrate (per Ramboll's recommendations);

- Zeroing ozone surface deposition in order to maintain elevated ozone concentrations and promote oxidant chemistry and associated aerosol formation (based on field measurements in the winter Uinta Basin reported by Helmig et al., [2014]).

In this project we investigated several specific hypothetical causes for the NH_3 shortfall in UDAQ's photochemical modeling application:

- The lack of a bidirectional surface-atmosphere NH_3 exchange in CAMx and any mitigating influence of snow cover on NH_3 deposition rates;
- Under estimates of on-road vehicle NH_3 emissions generated by the MOVES model, especially in the cold environment of SLC PCAP episodes;
- Potential under estimates of NH_3 emissions from various sectors, including livestock/agriculture, landfills, wastewater treatment, and residential wood combustion.

3.1 Replicating the UDAQ 2011 Base Case

UDAQ provided their entire modeling system to Ramboll, including their modified CAMx v6.3 source code (as described above), all model data inputs and outputs, key pre-processing scripts, 2011 $PM_{2.5}$ measurement data for model validation, all supporting files/datasets for SMOKE emissions processing, and all files associated with MOVES on-road emissions modeling. We ran the system using UDAQ's CAMx model for the December 31 – January 10, 2011 base case episode and confirmed that we successfully replicated UDAQ's results for each chemical species, in each grid cell of the two nested three-dimensional grids, during each hour of the modeling period, to within machine accuracy (single precision floating point differences within 1 in 10,000)[2].

3.2 Updating the Model Version

Ramboll publicly released CAMx v6.3 in 2016 when UDAQ began developing the SLC $PM_{2.5}$ modeling application. Since then we have released three subsequent CAMx versions that include several updates and improvements. In this study we applied the latest CAMx version (v7.0) to take advantage of these updates, including a new NH_3 bidirectional surface algorithm.

We conducted an initial "replication" run using CAMx v7.0 and compared results to v6.3 output to quantify impacts between the different model versions. We employed the same model configuration as v6.3; to ensure consistency, we also implemented the same UDAQ code modifications listed in Table 3-1. The only material differences from v6.3 included an update to SOA chemistry from SOAP v1 to SOAP v2.2 (Ramboll, 2020) and other minor updates to RADM and ISORROPIA aerosol chemistry introduced in v6.4. Given the small proportion of SOA relative to primary organic emissions in this case, the effects from the SOAP update were expected to be negligible, as were the updates to RADM and ISORROPIA. We verified that the update to v7.0 resulted in only inconsequential differences in $PM_{2.5}$ species concentrations relative to our v6.3 run. Specifically, v7.0 resulted in slightly higher organic aerosol, slightly lower inorganic secondary species, and zero differences in other primary $PM_{2.5}$, overall leading to insignificantly higher $PM_{2.5}$. We concluded from this replication run that there was no significant impact from updating the model version.

Figure 3-2 compares modeled 24-hour $PM_{2.5}$ species concentrations against measurements at two sites, Hawthorne and Lindon, on January 7 when total $PM_{2.5}$ concentrations peaked during the episode.

[2] When extracting and reporting gridded $PM_{2.5}$ results at the coordinates of monitoring sites, we were not able to reproduce UDAQ's extracted values. Subsequent investigation revealed that UDAQ applied a slightly different map projection to calculate grid coordinates at monitor locations; we verified that we could replicate UDAQ's results when using their coordinates for the Hawthorne $PM_{2.5}$ monitoring site. However, we have used our site coordinates for all analyses described in this report, and therefore results presented here differ somewhat from those presented in the SLC $PM_{2.5}$ SIP, MP and associated TSDs.

The figure is arranged to display component and total $PM_{2.5}$ in terms of both absolute concentrations and relative contributions. To make these comparisons, we converted CAMx total (primary plus secondary) organic aerosol (OA) concentrations to an organic carbon equivalent (OC) by dividing by 1.6 following UDAQ's approach. We then summed the CAMx non-carbon fraction of OA (i.e., OA-OC, containing oxygen, hydrogen, etc.) and non-crustal fine primary species (FPRM) to form the "Other" species shown in Figure 3-1. Finally, we mapped the CAMx fine crustal species (FCRS) directly to "Crustal" species in shown in Figure 3-1.

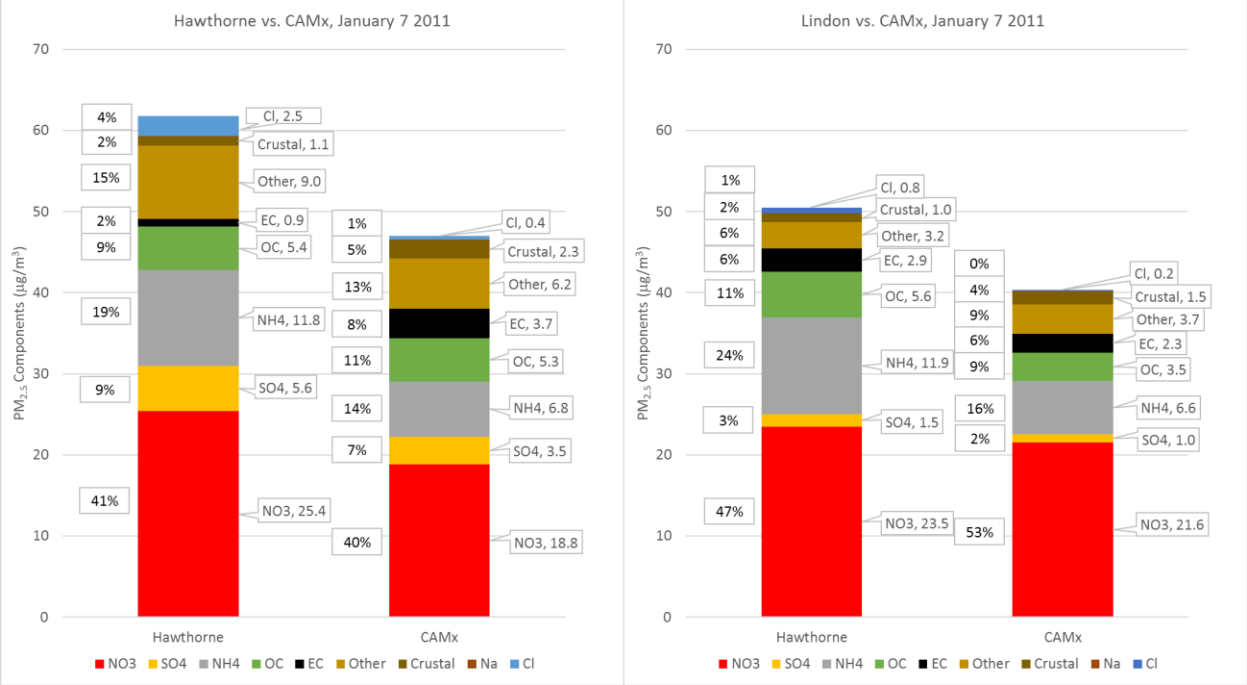

Figure 3-2. Comparison of modeled $PM_{2.5}$ species concentrations from the CAMx v7.0 replication run against measurements at Hawthorne (left) and Lindon (right) monitoring sites on January 7, 2011. Boxed values to the right of each stacked bar indicate the absolute concentration ($\mu g/m^3$) and boxed values to the left indicate percent contribution to total $PM_{2.5}$.

Generally, CAMx replicated the relative contributions of most species rather well but under predicted total $PM_{2.5}$ at both sites because of a lack of particulate NO_3 and associated NH_4. Sulfate and the minor contribution from particulate chloride (Cl) were also under predicted while the minor contribution from crustal was over predicted. Although sodium (Na) is included in the chart, it is not visible because concentrations were typically less than 0.1 $\mu g/m^3$. Figure 3-1 shows that the sum of elemental carbon (EC), OC and Other, which we can assume is nearly all associated with carbonaceous aerosol, was well replicated at both sites (15.3 $\mu g/m^3$ modeled vs. 15.2 $\mu g/m^3$ observed at Hawthorne, 9.5 $\mu g/m^3$ modeled vs. 11.7 $\mu g/m^3$ observed at Lindon). This suggests that the estimate of total carbon emissions from major primary carbon sources such as smoke is generally correct, but that the split among OA and EC emissions may need adjustment.

Table 3-2 lists statistical performance for individual 24-hour $PM_{2.5}$ species averaged over all three speciated monitoring sites (Hawthorne, Lindon, Bountiful) and all 10 monitored site-days when speciated measurements were available. We calculated normalized mean bias (NMB) and normalized mean unsigned error (NME) according to:

$$NMB = \frac{\sum(P_j - O_j)}{\sum O_j} \times 100$$

$$NME = \frac{\sum|P_j - O_j|}{\sum O_j} \times 100$$

where *P* represents a model prediction at site/day *j*, *O* is a measurement at site/day *j*, and the summation is over all site-days. NMB and NME are compared to statistical "criteria" recently compiled by Emery et al., (2016) to provide some context. These criteria indicate statistical values that most modeling applications documented in peer-reviewed literature over the past 15 years have achieved, while values beyond the criteria are considered poor performers for the particular metric. Note that certain species exhibited very large NMB and NME values, suggesting rather poor replication of measurements. However, the highest errors were associated with species that had small to negligible contributions to the $PM_{2.5}$ mass budget. When NMB was weighted by the measured relative contributions from each species (Table 3-3), the large errors in minor components were reduced substantially, revealing their actual insignificant contribution to overall $PM_{2.5}$ bias.

Table 3-2. Statistical performance for speciated and total 24-hour $PM_{2.5}$ concentrations over all measured site-days of January 1-10, 2011 for the initial CAMx v7.0 replication run. Statistical performance criteria from Emery et al. (2016) are also shown for context. Statistics within the criteria are displayed as green, those outside are displayed as red.

Species	NMB	NME	Criteria NMB	Criteria NME
NO_3	-37%	38%	<±65%	<115%
SO_4	-17%	33%	<±30%	<50%
NH_4	-47%	49%	<±30%	<50%
OC	-16%	29%	<±50%	<65%
EC	56%	75%	<±40%	<75%
Other	-49%	50%	N/A	N/A
Crustal	86%	102%	N/A	N/A
Na	143%	143%	N/A	N/A
Cl	-78%	78%	N/A	N/A
$PM_{2.5}$	-33%	35%	<±30%	<50%

Speciated measurement data were available on the following dates: Hawthorne: January 1, 5, 7, 9; Lindon: January 3, 5, 7, 9; Bountiful Viewmont: January 3, 9.

Figure 3-3 shows time series of modeled and measured total 24-hour $PM_{2.5}$ at six Federal Reference Method (FRM) monitoring sites in the Salt Lake and Utah Lake Basins. Table 3-4 presents $PM_{2.5}$ NMB and NME over the entire episode at each site and for the average among all sites. The model consistently under predicted $PM_{2.5}$ at all sites throughout the episode but tended to capture the inter-daily variations, which suggests that the simulated meteorology was generally capturing the build-up and cessation of the stagnant inversion pattern over the episode. Statistical performance was generally consistent among the monitoring sites, except for Brigham City and Ogden, which exhibited particularly large under prediction biases to the north of SLC. NMB and NME are numerically identical (different signs), indicating that all model error was associated with the systematic under prediction bias.

Table 3-3. Mass-fraction weighted contribution of species NMB from Table 3-2 to total $PM_{2.5}$ NMB. Average mass fractions are determined from all measured site-days.

Species	% $PM_{2.5}$ Mass	Weighted NMB
NO_3	43%	-16%
SO_4	5%	-1%
NH_4	18%	-8%
OC	10%	-2%
EC	3%	2%
Other	17%	-8%
Crustal	2%	2%
Na	0%	0%
Cl	3%	-2%
$PM_{2.5}$	100%	-33%

Table 3-4. Statistical performance for total 24-hour $PM_{2.5}$ concentrations at FRM sites in the Salt Lake and Utah Lake Basins over January 1-10, 2011 for the initial CAMx v7.0 replication run.

FRM Site	NMB	NME
Hawthorne	-31%	31%
Lindon	-33%	33%
Bountiful	-35%	35%
Brigham City	-67%	67%
Ogden	-42%	42%
Tooele	-27%	27%
All Sites	-37%	37%

Figure 3-4 shows time series of modeled and measured hourly gas concentrations at the Hawthorne monitoring site. Table 3-5 presents hourly gas NMB at the same site over the entire episode. Carbon monoxide (CO) is a good tracer for combustion sources and given its slow rate of oxidation can be considered practically inert in this situation. Therefore, CO is useful to assess the combination of estimated emissions and simulated dispersion. Up through January 7, simulated CO was out of synch with observations, as the model was too low on high CO days and vice versa. This implies poor replication of inversion strength/depth, dispersion patterns and/or inaccuracies in allocating daily CO emissions spatially and temporally. However, peak CO over the period was comparable to measurements and Hawthorne NMB over the entire episode is practically zero, indicating that daily CO emissions were generally well-quantified.

Nitric oxide (NO) is directly emitted from combustion sources and is transformed to nitrogen dioxide (NO_2) depending on the availability of ozone (O_3). NO tended to be under predicted, especially on January 5 and 6 when observed NO reached very high levels (100-250 ppb) in the night and morning hours as seen for CO. This indicates that either (1) simulated NO emissions were too low, (2) there was insufficient stagnation to build up NO, and/or (3) modeled O_3 was abundant to transform NO to NO_2. But simulated NO_2 also exhibited an under prediction tendency, and as seen in the NOx plot

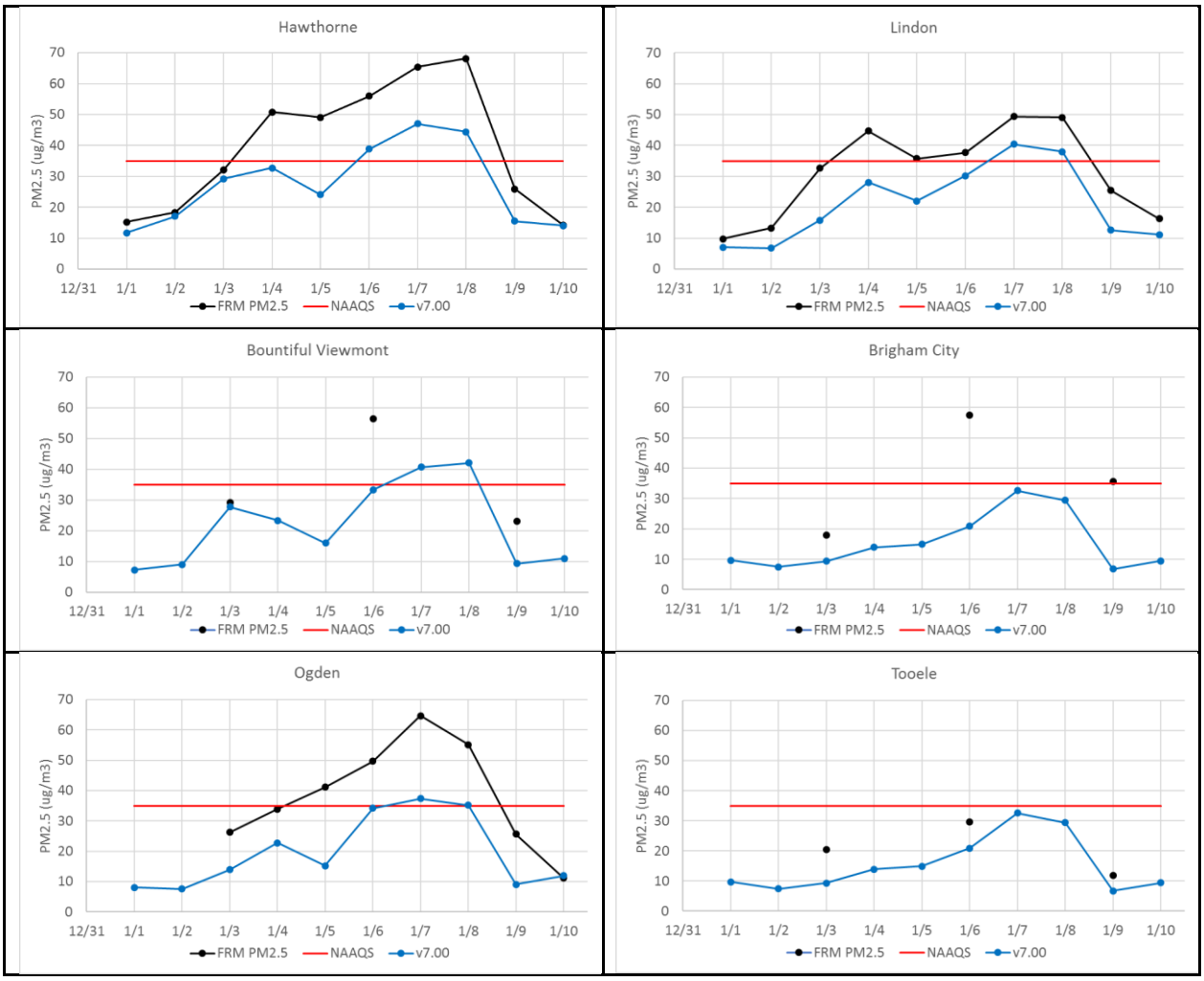

Figure 3-3. Time series of modeled (blue) and measured (black) total $PM_{2.5}$ at six FRM sites in the Salt Lake and Utah Lake Basins. The 24-hour $PM_{2.5}$ standard is shown as the horizontal red line.

Table 3-5. Statistical performance for hourly gas concentrations at the Hawthorne monitoring site over January 1-10, 2011 for the initial CAMx v7.0 replication run.

Gas Species	NMB
Carbon Monoxide (CO)	1%
Nitric Oxide (NO)	-50%
Nitrogen Dioxide (NO_2)	-30%
Nitrogen Oxides (NOx)	-40%
Ozone (O_3)	125%
Odd Oxygen (Ox)	5%

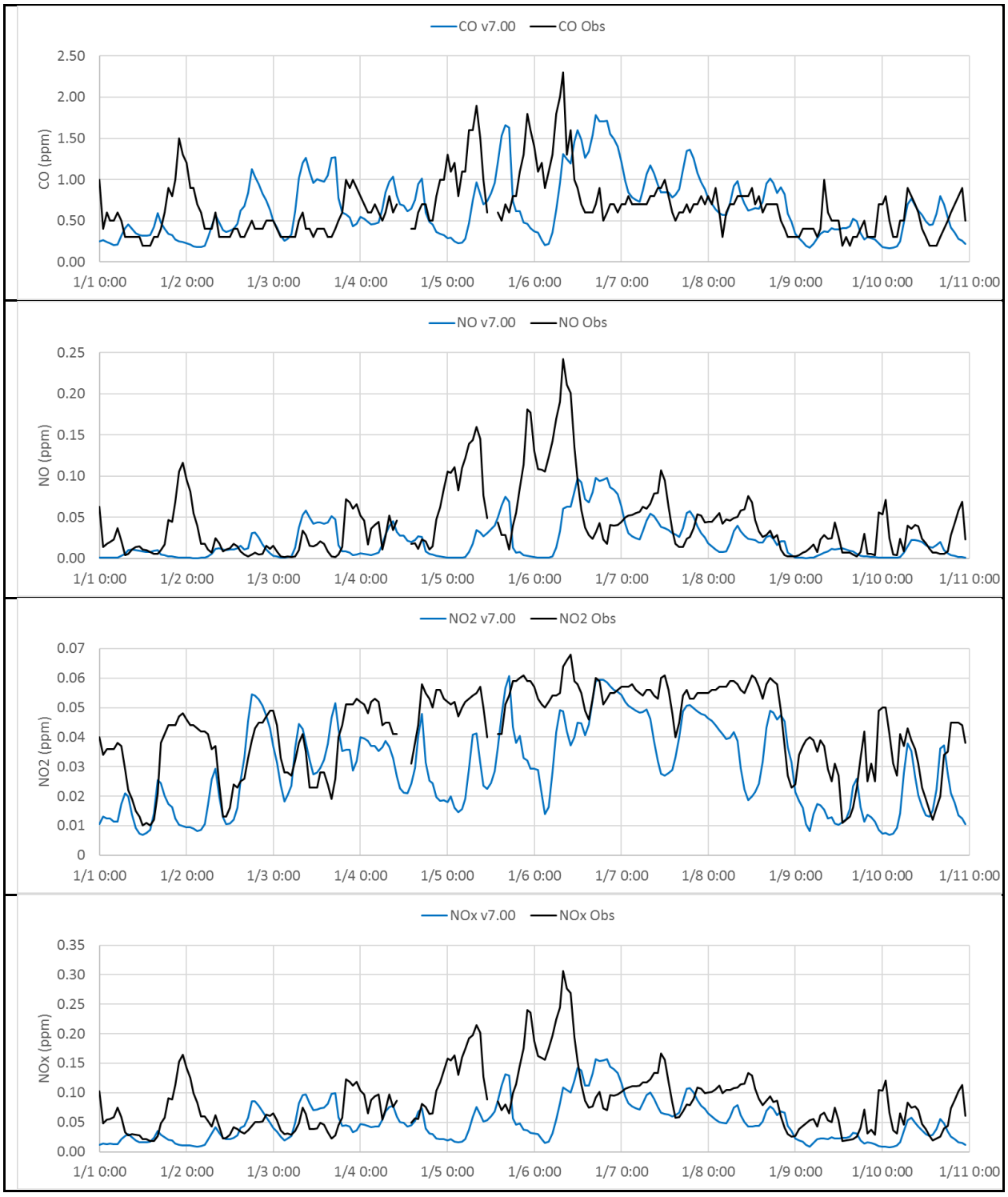

Figure 3-4. Time series of modeled (blue) and measured (black) hourly gases at the Hawthorne monitoring site. Measurements of NH_3 are unavailable and modeled results are shown for context.

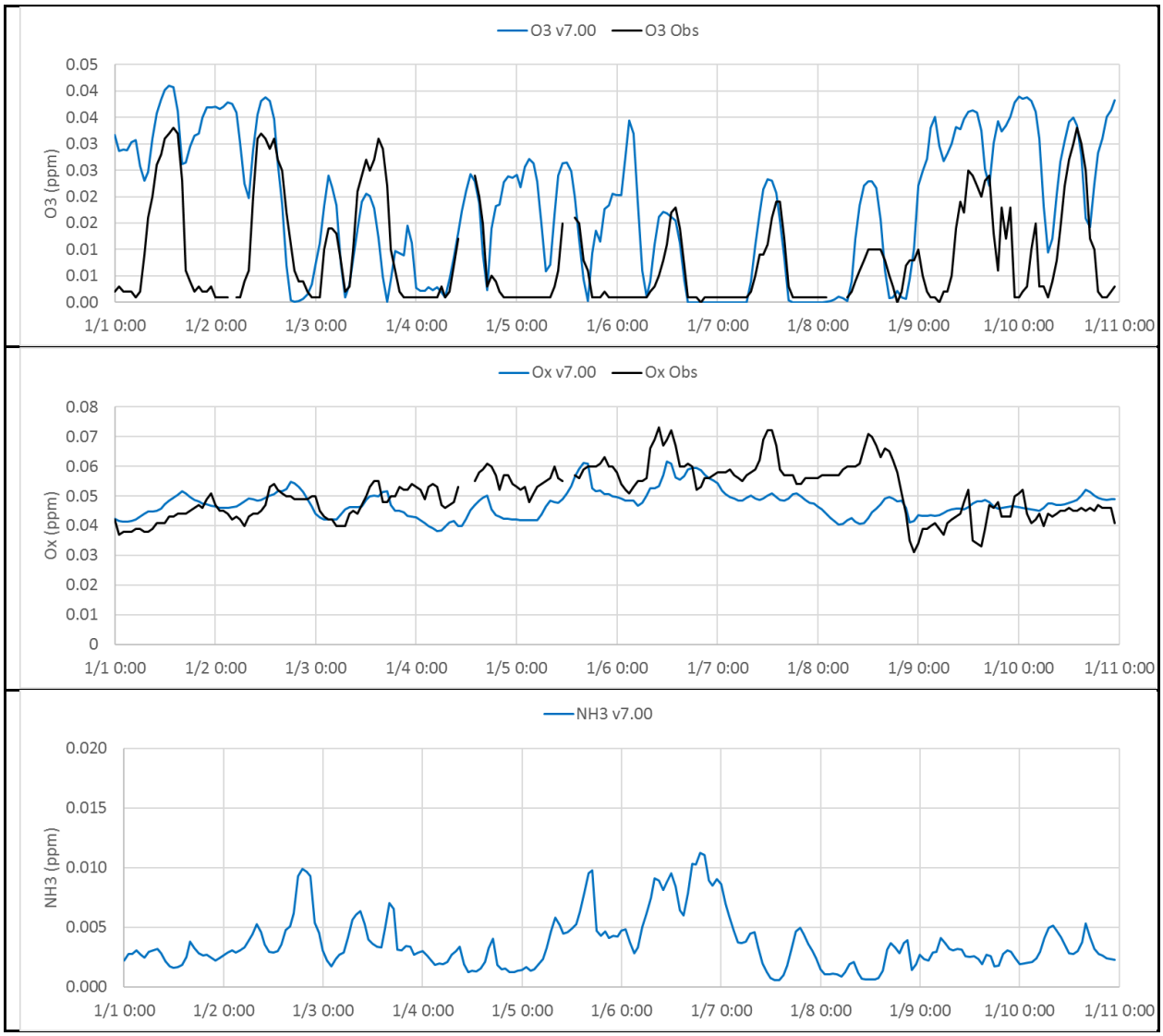

Figure 3-4 (concluded).

($NO+NO_2$), there was insufficient NOx buildup at Hawthorne. These leaves only (1) and (2) as viable causes for low NOx concentrations.

Time series for simulated O_3 tended toward observed conditions during the middle of the episode when $PM_{2.5}$ peaked, but generally O_3 was over predicted during the midday and throughout inversion build-up and cessation. The model correctly simulated the complete chemical removal of O_3 during certain mid-episode night and morning hours as it reacted with NO to form NO_2. Odd oxygen (Ox = NO_2 + O_3) allows us to evaluate the chemical processing between NOx and O_3. During mid-episode, Ox transitioned from slight over predictions to under predictions. It was particularly low on January 7 and 8 when the largest under predictions of $PM_{2.5}$ and nitrate occurred – this establishes a link relating low rates of NOx oxidation and the lack of nitrate production.

Finally, simulated NH_3 concentrations ranged from a few ppb to a peak of 10 ppb during the highest $PM_{2.5}$ days, with an episode average of ~4 ppb. This simulated range was consistent with past

measurements at one site in February 2016 as presented in the UDAQ MP. However, it was roughly a third of the average 11-12 ppb measured in SLC during the February 2019 WaFACO study.

In summary, details in temporal/spatial allocation and/or a poor characterization of inversion depth/strength and dispersion patterns may have caused a poor replication of measured CO time series, under predictions of NOx and over predictions of O_3, particularly during the middle of the episode. Obviously, the same meteorological issues influence simulated NH_3 patterns. The lack of NOx may also be caused in part by emission under estimates, and according to Ox patterns, the model lacks NO_2 generation and therefore likely further oxidation to NO_3. Additional chemical processing would help generate more NO_3 on highest $PM_{2.5}$ days.

4.0 TESTING MODEL IMPROVEMENTS

This section describes the numerous model tests that Ramboll conducted with CAMx v7.0 to assess sensitivity to various improvements that we identified based on review of UDAQ's modeling configuration, modifications, emission inputs, and CAMx performance against available measurements.

4.1 Physical Processes

4.1.1 Vertical Mixing

As described in Section 3, UDAQ increased vertical mixing rates and depths early during the development of their modeling configuration. Specifically, UDAQ achieved this by setting minimum vertical diffusion coefficients, or "diffusivities", in urban areas to levels that ensure some mixing through the lowest 600 m (~2000 ft) throughout all hours of the episode. This amount and depth of mixing is excessive when considering that under stagnant, strong inversion conditions emissions should be trapped in a shallow (100-200 m) urban surface boundary layer. Over mixing in the model is evident from the time series of gas concentrations shown in Section 3: CO and NOx under predictions indicate too much upward mixing of emissions, and excessive O_3 indicates too much downward mixing of O_3 from aloft. UDAQ increased mixing rates around the same time they increased NH_3 emissions and so it is possible that the NH_3 emissions shortfall, and thus the amount added to the emission inventory, were over estimated. In other words, the same chemical improvement may be achieved with a lower quantity of NH_3 emitted into a shallower mixed layer.

We conducted two model tests to identify an optimum level of diurnal mixing that minimized the NH_3 shortfall without negatively impacting model-measurement agreement for other precursor gas and $PM_{2.5}$ component concentrations. We reduced minimum (nighttime) urban boundary layer depths to more physically appropriate values of 100 and 200 m. This change improved under predictions of the major secondary PM species (NO_3, SO_4, NH_4), OC, Other mass, total $PM_{2.5}$, NOx, and NH_3 (by 5-10 ppb) at all sites, while slightly worsening over predictions of the minor primary $PM_{2.5}$ components EC and Crustal. Ozone over predictions slightly improved while CO exhibited more over predictions, especially during nighttime hours. $PM_{2.5}$ increased by more than 10 $\mu g/m^3$ on some days at Hawthorne. Since only urban mixing was impacted in both the UDAQ configuration and in these tests, there were negligible to zero impacts at more rural sites such as Tooele where $PM_{2.5}$ remained quite low.

Conclusion: We continued to apply reduced vertical diffusion rates for all remaining simulations.

4.1.2 Dry Deposition and Bi-directional Surface NH_3 Exchange

The CAMx photochemical model includes the process of "dry deposition", which refers to diffusive transfer of gases and particulates from the model's lowest atmospheric layer to the surface. This process is analogous to the flow of electric current through resistors along a circuit. Dry deposition normally addresses the irreversible uptake of those compounds by surface elements (vegetation, soil, water, snow) according to chemical-specific attributes. Until recently, the CAMx dry deposition process has been strictly a removal process for all chemical species, based on the approach of Zhang et al. (2003). Ramboll has recently added the bidirectional NH_3 algorithm of Zhang et al. (2010) and Whaley et al. (2018) to CAMx v7.0. Implemented directly within the dry deposition function, the new approach assigns NH_3 "emission potentials" by land cover type that determine temperature-dependent compensation points along the circuit (Figure 4-1) and thus the direction and magnitude of the net NH_3 exchange between the lowest atmospheric model layer and surface elements. Under conditions of high

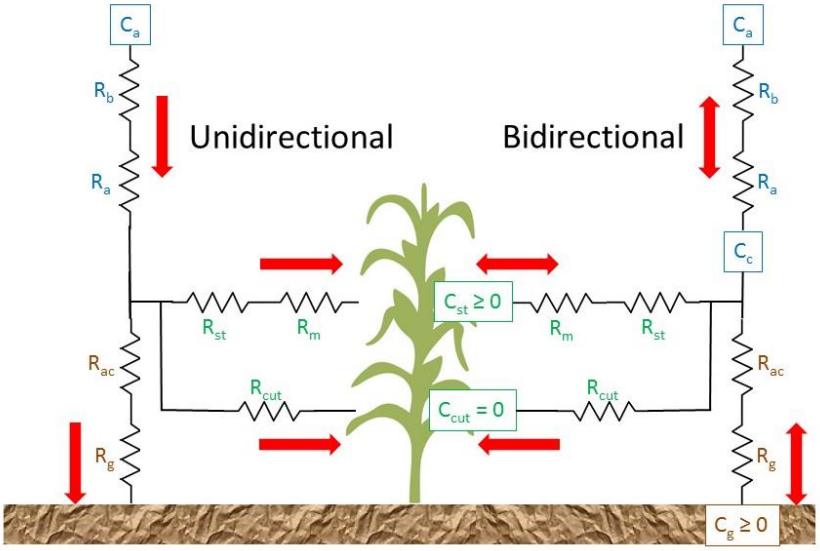

Figure 4-1. Right side shows a schematic of the bidirectional NH_3 deposition/re-emission scheme of Zhang et al. (2010) and Whaley et al. (2018); left side shows the original unidirectional deposition scheme of Zhang et al. (2003). Respective pathway resistances (R) and bidirectional compensation points (C) are shown.

compensation points relative to atmospheric concentrations, the net exchange is from the surface to the atmosphere, i.e. emission; when atmospheric concentrations are high relative to the compensation points, the net exchange is to the surface, i.e., deposition. In all cases with non-zero emission potential, NH_3 deposition rates to the surface are reduced (or reversed) relative to the original deposition function that implicitly assumes zero emission potential. Therefore, use of the bidirectional NH_3 process can potentially increase the buildup of atmospheric concentrations.

We invoked the Zhang bidirectional scheme using default emission potentials by landcover type according to Whaley et al. (2018). To our initial surprise, we found that NH_3, NH_4, particulate NO_3, and $PM_{2.5}$ concentrations were not impacted. Based on review of the Zhang source code, we found that snow cover defeats the bidirectional treatment for all land cover types except for a few categories with large wintertime leaf area index that extend above the snow (e.g., pine forests, which are assigned small emission potentials and well removed from the central basin).

In fact, additional CAMx tests revealed that the Zhang scheme actually increases NH_3 deposition rates into snow relative to no-snow conditions because daytime snow melt absorbs more of this very soluble compound into surface liquid water. The bidirectional scheme is unable to account for release of NH_3 from snow when it refreezes at night. Scientific literature on NH_3 surface exchange confirms that such a "breathing" process occurs during the formation and evaporation of liquid dew (Wentworth et al., 2016). We could not find any clear signs for actual diurnal deposition/release of NH_3 from snow according to plots of winter 2016 time series measurements at Neil Armstrong Academy (UDAQ, 2020a). Based on informal inquiries to several nitrogen deposition experts there seems to be little common knowledge on the interaction of snow cover and NH_3 re-emission.

We repeated the bidirectional NH_3 test but with the mitigating effect of snow cover removed to identify the largest potential effect of the scheme. This resulted in small (less than 1 $\mu g/m^3$) increases in ammonium nitrate on some days. So even without snow cover, the default configuration of the bidirectional scheme did not significantly alter simulation results.

Conclusion: The presence of snow cover squelches bidirectional NH_3 surface exchange, and in fact enhances surface NH_3 deposition. The maximum potential impact of the CAMx bidirectional scheme in this particular application was insignificant to minor as currently configured and indicated a relatively minor role for surface NH_3 exchange (deposition or re-emission) in the absence of snow cover. We decided to drop this option in all remaining simulations.

4.2 Emission Processes

According to the MP, UDAQ estimated county-level NH_3 emission shortfalls from model-measurement concentration differences throughout the SLC NAA and then added those additional emissions uniformly over all hours and across all grid cells representing the basin floor within each county regardless of land cover type. As we understand it, the rationale for this methodology assumed that the NH_3 shortfall is from unknown, potentially un-inventoried sources and thus no a priori knowledge exists about its spatial or temporal distribution. However, enhanced vertical mixing coupled with the expansive area to which additional NH_3 emissions were applied resulted in a massive volume and thus the need for a very large quantity of additional NH_3. UDAQ reports that the artificial NH_3 injection comprised ~40% of the final Salt Lake County total emissions going into the model, meaning that the injection added ~65% to the original episodic emission inventory. We began this project with the expectation that one to several inventoried NH_3 sources are likely under estimated and thus would be confined to the areas where such activity occurs.

Given the large number of source types that emit NH_3, and the widely dispersed nature of many of those sources, pinpointing the causes for the NH_3 emissions shortfall is challenging. Agricultural activity is often identified as the largest source, and this remains true in rural areas to the north and south of SLC. Agricultural lands in the NAA have given way to urban sprawl and commercial/industrial uses. Other than agricultural sources, on-road vehicles comprise the largest NH_3 source in the basin.

To reassess the modeled NH_3 shortfall after reducing vertical mixing rates, we removed UDAQ's artificial NH_3 emissions from the CAMx emission input files and re-ran the model. Generally, concentrations of NH_4, particulate NO_3 and SO_4 were reduced back to levels a bit lower than the CAMx v7.0 replication run (i.e., with deep mixing) with no impact on other PM species.

Conclusion: This run confirms that additional NH_3 emissions are needed in the model but reducing vertical mixing to more reasonable levels reduces the NH_3 shortfall.

4.2.1 On-Road Vehicle Emissions

According to the UDAQ 2011 modeling inventory, on-road vehicles are the dominant winter source of emissions in the SLC NAA. Light-duty gasoline vehicles represent the overwhelming fraction of vehicles, and their NH_3 emission rates have been investigated over many years. Past surveys suggest several conditions that are present in Utah can increase NH_3 emission rates, including high load demands such as climbing grades and acceleration events, cold conditions, and aged vehicles (Durbina et al., 2004). Diesel vehicles with Selective Catalytic Reduction (SCR) equipment inject urea into the exhaust system that thermally decomposes to NH_3 to reduce NOx emissions. SCR technology has been evolving since the 2010 model year when diesel NOx emission standards first required SCR. SCR catalysts are inefficient below 200°C and NH_3 may "slip" through the catalyst. There are a variety of heavy-duty engine aftertreatment control designs and operating programs that affect average NH_3 emission rates.

Tailpipe NH_3 emission factor estimates in EPA's MOVES2014 model were developed with data from well before 2014. The data available to EPA at that time may not have been able to fully address all

conditions, including cold weather, aging or unmaintained vehicles, unique driving activities, and the latest diesel vehicles using SCR. There are published studies (Sun et al., 2014, 2016) indicating that light-duty vehicle NH_3 emissions may be under estimated by a factor of two under "normal" conditions. While this discrepancy may be related to the age of data upon which MOVES is based, it is also possible that even more NH_3 may be emitted under conditions specific to Utah.

Ramboll conducted a literature review of several publications addressing on-road vehicle NH_3 emission measurements. Appendix A presents results from our review. Results for light-duty gasoline vehicles show that aged vehicles, surface street operation and aggressive driving patterns produce substantially higher NH_3 emissions relative to standard test methods upon which the MOVES model is based. Cold starts and cold conditions could result in higher NH_3 emissions as well: measurements at -7°C (20°F) resulted in a 28–47% increase over those at 22°C (72°F). A larger impact occurs for engine load, where just a small percentage of grades or high acceleration modes can cause emission increases by orders of magnitude (Huai et al., 2003). For example, high power test cycles produce 5.5 times more NH_3 than standard (lower power) test cycles. Diesel vehicles generate NH_3 emissions only when equipped with SCR equipment. To meet NOx emissions standards SCR was installed only in post-2007 light-duty and post-2010 heavy-duty vehicles. Given the small penetration of SCR into the diesel fleet in 2011, our review indicates that a much larger proportion of NH_3 emissions uncertainty in 2011 is related to light-duty gasoline vehicles, particularly those fleets that include a high proportion of aged vehicles operating in cold conditions. In 2020, a much larger proportion of diesel vehicles are equipped with SCR and so MOVES should reflect higher NH_3 emissions from that sector in UDAQ's future year emission inventory projection.

We conducted an in-depth review of 2011 day-specific non-diesel exhaust NH_3 emission factors and normalized emission rates (mass of NH_3 emitted per energy produced) generated by UDAQ's application of the MOVES2014 model and compared them to the published results summarized in Appendix A. The separate effects from cold temperatures and high-load activity (i.e., climbing grades) were not included, and so this analysis just compared emissions under "normal" conditions. From this analysis, we developed NH_3 scaling factors by county (Box Elder, Davis, Salt Lake, Tooele, Utah, Weber), road type (rural and urban, restricted and unrestricted access), vehicle type (motorcycle, passenger car and truck, several truck types, buses, motorhomes) and fuel type (gasoline, ethanol [E85], and compressed natural gas [CNG]) to account for different activity and published emission rates across these four dimensions. We assumed that local gasoline contains 10% ethanol. We applied the resulting matrix of factors to UDAQ's on-road mobile emission files that are processed by SMOKE to generate temporally and spatially resolved emission inputs for CAMx. Table 4-1 lists the net NH_3 scaling factors by county that account for the mix of activity across all vehicle, fuel, and roadway types. Larger factors were calculated for urban counties because of the higher activity fraction for gasoline, ethanol and CNG vehicles. While the UDAQ NH_3 injection added ~65% to the original Salt Lake County episodic emission inventory, the on-road NH_3 increase added ~40%.

Table 4-1. Net NH_3 emission scaling factors developed from comparing 2011 normalized emission rates from MOVES2014 to published results summarized in Appendix A.

County	NH_3 Factor
Box Elder	1.749
Davis	2.034
Salt Lake	2.156
Tooele	1.963
Utah	2.117
Weber	2.274

We re-ran CAMx with the scaled on-road NH_3 emissions in lieu of UDAQ's NH_3 injection; this run continued to use reduced vertical diffusion rates. We will refer to this CAMx run as "MV NH_3 Emissions" in the remainder of the report. Figure 4-2 displays model-measurement comparisons of total $PM_{2.5}$ at FRM sites similar to those presented in Section 3.2. Particulate NO_3 and NH_4 concentrations increased substantially relative to the no-injection run described above, but not quite up to levels achieved with the NH_3 injection. These results show that the model simulated a NH_3-limited (sensitive) environment, since particulate NO_3 responded significantly by removing and adding NH_3 emissions. Total $PM_{2.5}$ concentrations at Hawthorne and Lindon improved over the CAMx v7.0 replication run but were slightly lower than the replication run at other FRM sites. Gas NH_3 concentration time series also exhibited a substantial increase over the no-injection run, in better agreement with recent measurements, so not all NH_3 went into particulate NO_3. This indicates that as more NH_3 is added, gaseous NH_3 may increase at a relatively larger rate than particulate NH_4 and NO_3, indicating a shift toward a balance between NH_3-limited vs. NO_3-limited conditions. Small and infrequent increases in sulfate indicated that more NH_3 also affected aqueous sulfate production by reducing cloud acidity, thereby making aqueous production more efficient.

Figure 4-2. Time series of CAMx v7.0 replication run (blue), CAMx "MV NH_3 Emissions" run (orange), and measured (black) total $PM_{2.5}$ at six FRM sites in the Salt Lake and Utah Lake Basins. The 24-hour $PM_{2.5}$ standard is shown as the horizontal red line.

Figure 4-3 compares NH_3 concentration patterns averaged over the February 2019 WaFACO study to modeled NH_3 concentrations averaged over January 3-8, 2011, from the "MV NH_3 Emissions" run described above. The model reproduced spatial patterns rather well throughout the Wasatch Front modeling domain. In the Salt Lake Valley, maximum concentrations aligned with population density along the I-15 corridor and in central SLC, showing the dominance of on-road and commercial/industrial sources. By visual inspection, average modeled NH_3 concentrations in the core urban area of SLC appear to be well-represented but low by roughly 5 ppb. Measured NH_3 patterns in Davis, Weber and Utah Counties indicate the dominance of agricultural emissions, where the model under predicts NH_3 by more than a factor of 2. This lack of NH_3 could explain much of the $PM_{2.5}$ under predictions at Ogden and Brigham City. There remain continued under predictions of ammonium nitrate, and field measurements suggest other important sources that appear to be lacking in the modeling inventory. In the sub-sections that follow, we have compared information inferred from NH_3 measurements to the UDAQ NH_3 emission inventory.

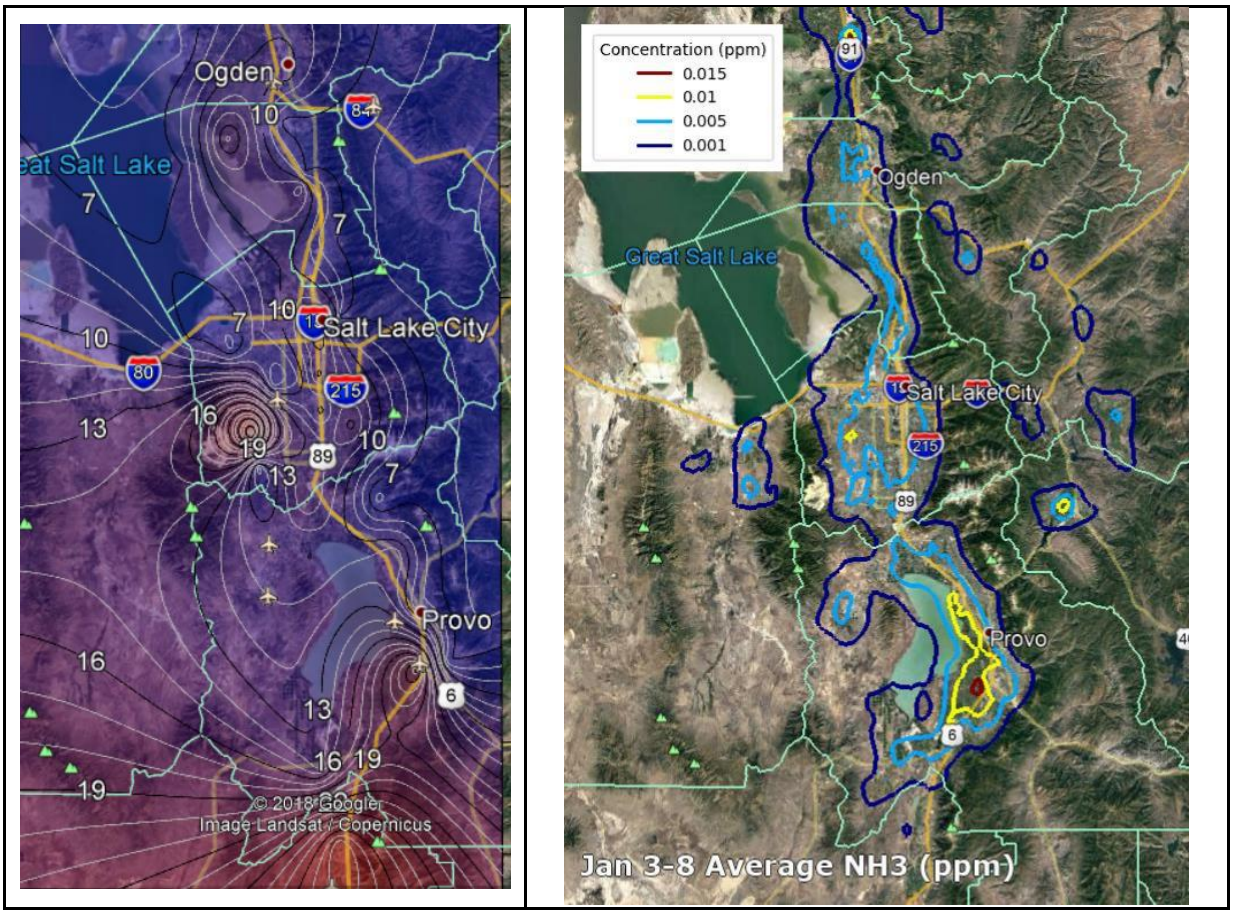

Figure 4-3. Left side shows the spatial distribution of measured NH_3 (ppb) averaged over the February 2019 WaFACO field study. Right side shows the spatial distribution of CAMx simulated NH_3 (ppm = ppb/1000) averaged over January 3-8, 2011 for the "MV NH_3 Emissions" run.

Conclusion: Scaling up on-road NH_3 emissions resulted in improved agreement with speciated $PM_{2.5}$ measurements over the no-injection case, but the model continued to under predict ammonium nitrate. In this case, the modeled PM nitrate response was NH_3-sensitive.

4.2.2 On-Road Vehicle Emissions in Cold Weather

As described above and in Appendix A, there is scientific literature evidence that on-road NH_3 emissions may increase by up to ~50% in freezing conditions. We conducted a follow-on CAMx sensitivity test where we scaled up on-road vehicle NH_3 emissions by an additional 40% over the increased emissions described in Section 4.2.1. We estimated this particular percentage based on the fraction of gasoline vehicles operating in the Wasatch Front. The objective of this test was to verify if a plausible amount of additional NH_3 emissions result in more PM nitrate or if the model chemistry transitions toward a neutral or nitrate-limited environment.

In this case, $PM_{2.5}$ increased by an additional ~2 $\mu g/m^3$ at Hawthorne, Bountiful and Ogden during the peak of the episode (January 7 and 8), comprising minor increases among particulate NO_3, SO_4 and NH_4. Ammonium nitrate under predictions persisted on these days – small effects for such a large rise in NH_3. In fact, the peak additional 24-hour NH_4 at Hawthorne (0.4 $\mu g/m^3$ on January 7) was far less than the additional 24-hour NH_3 at Hawthorne on the same day (2.5-3.7 ppb or 1.6-2.3 $\mu g/m^3$) by about a factor of 5.

Conclusion: These results confirm a shift towards NO_3-limited chemistry. The model predicts about the right amount of SO_4 and is approaching the right amount of NH_3 in the SLC basin (based on comparisons to 2019 measurements). The model continues to lack particulate NO_3 by about 30%, which is consistent with if not generally better than other $PM_{2.5}$ modeling applications in the western US.

4.2.3 Scaling Up NOx Emissions

Evidence from the tests above indicated that there was insufficient NOx from which to derive nitrate. Over the entire episode the model under predicted NOx at Hawthorne by about 15% while the diurnal patterns were not in synch with measurements (like CO). We tested the hypothesis that more NOx would generate more NO_3 by scaling up all gridded NOx emissions by 20%; point source NOx was not modified as those emissions are well-defined, not widely dispersed throughout the basin, and minor relative to the entire NOx inventory. This test included both additional increases in on-road vehicle NH_3 emissions described above (100% for "normal" conditions, 40% for cold conditions).

This CAMx test resulted in mostly decreases in $PM_{2.5}$ concentrations at the SLC and Lindon monitoring sites, by 1.5-2 $\mu g/m^3$, relative to the run described above in Section 4.4.2. $PM_{2.5}$ reductions mostly resulted from lower particulate NO_3 and NH_4, and OC also decreased by a very small amount (less than 0.05 $\mu g/m3$) at these sites. Positive but negligible increases in $PM_{2.5}$ resulted at Brigham City, Ogden and Tooele. We verified that NOx concentrations increased by ~20% while O_3 decreased daily by 5-10 ppb, in better agreement with measurements.

In the SLC urban zone, the addition of NOx in an already NOx-rich modeled environment (relative to VOC) further squelched oxidant chemistry and reduced production of NO_3 and SOA. Further, less particulate NO_3 confirmed NO_3-sensitivity in the modeled urban zone. The minor $PM_{2.5}$ increases in the outer areas indicated that those modeled environments remained photochemically NOx-sensitive (more efficient oxidation) and so slightly more NO_3 was generated.

Conclusion: The addition of sufficient NOx emissions to remove an episode-average NOx under prediction bias resulted in lower $PM_{2.5}$, particulate NO_3 and NH_4 in the SLC urban area, and thus such NOx increases are unwarranted. This further indicates that the model simulates a NOx-disbenefit environment both in terms of oxidant chemistry and $PM_{2.5}$ formation. Additionally, this run confirmed that PM nitrate formation varies between NOx-sensitive and NH_3-sensitive over the episode.

Collectively, the sensitivity tests conducted to this point strengthen evidence for the following remaining issues:

6. The model's inability to sufficiently convert NOx to nitrate is caused by a chemical limitation – some possible causes are addressed in Section 4.3 below;
7. As previously discussed in Section 3.1, the meteorological dispersion patterns are not well replicated, limiting the ability to build up secondary $PM_{2.5}$;
8. Daily emissions are not correctly allocated in space and time – other key emission sectors are addressed below.

4.2.4 Area Sources

Measurements taken during the 2019 WaFACO study exhibit high localized NH_3 concentrations, often approaching 1000 ppb, around active livestock facilities such as dairy farms in Davis, Weber and Utah Counties (as evident in Figure 4-3). We investigated emission estimates for agricultural emissions in the UDAQ 2011 inventory, along with their assigned spatial and temporal allocation. We confirmed that livestock waste is the largest agricultural emissions sector in the winter inventory, while fertilizer application related to crop activities is minimal as expected. In developing model-ready emission files, UDAQ distributes county-level agricultural emissions to general agricultural land use for certain livestock sectors (cattle, swine, poultry, sheep) but we found that other livestock sectors (goats, turkey production, horses/ponies) are assigned to population density. We also confirmed that no livestock emissions are allocated to specific animal husbandry facility locations. Other than the spatial allocation issue, we found no obvious problems with seasonal allocation or annual emission rates.

We also investigated residential wood combustion (RWC) as a possible source of NH_3 uncertainty. UDAQ provides documentation on how RWC emissions were estimated on a daily basis. Based on rather good model performance for $PM_{2.5}$ species components that are dominated by wood smoke (EC, OC and Other) we believe that RWC activity, temporal and spatial allocation, and associated PM emission estimates are well characterized in the model. However, it is possible that NH_3 emission factors could be in error. According to the UDAQ emission inventory, RWC NH_3 ranges 10-100 times less than on-road vehicle NH_3 emissions. Any errors in RWC NH_3 emission factors would need to rival on-road emissions to have any effect on simulated NH_3 concentrations, which is implausible.

Conclusion: There are very likely large emission uncertainties associated with the major winter-time NH_3 area source sector (livestock waste). In the more rural counties of Box Elder, Weber, Tooele, and Utah under estimates of agricultural NH_3 could be the primary cause for $PM_{2.5}$ under predictions. In SLC, large errors in these sectors (even by factors of 10) would be small relative to total on-road vehicle emissions. We did not modify the area source inventory to address NH_3 from agriculture, because of a lack of information on emission factors, livestock type and headcounts, and spatial allocation to the modeling grid. According to evidence from the 2019 winter field study, no additional significant area emission discrepancies are apparent.

4.2.5 Point Sources

Measurements taken during the 2019 WaFACO study exhibit high localized NH_3 concentrations around large solid waste landfills, apparently from composting operations. The most significant of these is the Trans-Jordan landfill in the southwest Salt Lake County, as seen by the large measured concentration peak in Figure 4-3. This source is entirely missing in the model's emission inventory. Other landfills exist just south of I-80 west of the I-15 corridor. In fact, the UDAQ modeling inventory reports zero county-level NH_3 landfill emissions and includes only one point source facility with non-zero NH_3 emissions located in Davis County near Hill Air Force Base (0.03 TPD). We found that county-level landfill emissions are assigned to the wide-spread agriculture spatial surrogate in SMOKE processing.

Especially with the recent increase in composting activities, landfills are likely major localized sources throughout the basin.

USU found no obvious NH_3 emissions near wastewater treatment facilities and we confirmed there are no NH_3 emissions for this sector reported in the UDAQ emission inventory. We found a single water reclamation facility listed in the UDAQ point source inventory, located in central SLC, but its NH_3 emissions are set to zero. A Google search reveals several facilities along the I-15 corridor through Salt Lake County generally following river drainage to the Lake. We found that county-level wastewater treatment emissions are assigned to the population spatial surrogate in SMOKE processing.

Conclusion: According to field measurements, NH_3 emissions from landfills are likely under reported in the UDAQ inventory yet appear to have a significant localized impact. We did not modify the point source inventory to address NH_3 from landfills because of a lack of information for this sector. Although we identified wastewater reclamation as a potential issue early in the project, this was not apparent in the field measurements and no NH_3 emissions are reported in the UDAQ inventory for this sector. According to evidence from the 2019 winter field study, no additional significant point emission discrepancies are apparent.

4.3 Chemical Processes

Evidence from CAMx sensitivity tests to this point indicated that increased NH_3 emissions helped to improve model performance for ammonium nitrate, but further NH_3 increases pushed the chemical environment to neutral or NO_3-limited conditions. We conducted additional CAMx tests to investigate sensitivities related to the chemical production of NO_3 from NOx and the inorganic equilibrium between secondary acids and neutralizing cations.

4.3.1 Inorganic PM Treatment

CAMx v7 includes two inorganic PM thermodynamic algorithms: the original ISORROPIA v1.7 (Nenes et al., 1998, 1999) and EQSAM4clim (Metzger et al., 2016). ISORROPIA was used throughout all of UDAQ's modeling and all of Ramboll's CAMx runs described so far. EQSAM is a new simpler parameterization developed by statistically consolidating results from the fully explicit ISORROPIA algorithm. In this test, we substituted ISORROPIA with EQSAM to understand the choice of algorithm on nitrate performance. This resulted in slightly lower inorganic secondary $PM_{2.5}$ concentrations, especially for nitrate, leading to noticeably lower $PM_{2.5}$ on some high observed days such as January 7.

Conclusion: We continued to use ISORROPIA for all remaining simulations.

4.3.2 The Role of Nitryl Chloride

The CB6r2h gas-phase chemistry in CAMx includes the formation of nitryl chloride ($ClNO_2$) and nitric acid via heterogeneous nighttime reactions among hydrochloric acid (HCl) and N_2O_5, and the subsequent daytime photolysis of $ClNO_2$ generating NO_2 and chlorine radicals. UDAQ postulated that a lack of chloride in the model, relative to what is typically observed, may limit the simulated oxidation of NOx to NO_3. There is a large, well-documented industrial chloride source on the west side of the Salt Lake, which could contribute to higher than typical PM chloride levels that could enhance oxidant chemistry in the basin. However, simulated wind fields during the modeling episode do not bring the chloride plume across the Lake and up against the Wasatch Front to the extent that such chloride chemistry would be substantially impactful in the urban areas (UDAQ, 2020a).

We conducted a very simple CAMx sensitivity test to investigate the role of chloride chemistry on $PM_{2.5}$ levels, focusing on particulate Cl (which is also under predicted) and the formation of nitrate. Given the lack of chloride emission in the urban corridor, we set an artificial lower bound for HCl concentrations at 0.1 ppb in order to maintain elevated chloride levels throughout the domain. The basis for our choice of 0.1 ppb was guided by the findings from Riedel et al. (2013), who analyzed wintertime $ClNO_2$ and Cl_2 measurements on a 300 m tall tower in Colorado. From their results specific to Denver urban plume impacts, we expected to produce $ClNO_2$ at a few tenths of 1 ppb.

Results from this test showed mixed minor $PM_{2.5}$ impacts. Small nitrate reductions were balanced by small increases in SO_4 and NH_4. Markedly higher particulate Cl concentrations resulted in improved agreement with Hawthorne measurements. For example, modeled Cl at Hawthorne on January 7 increased from 0.42 $\mu g/m^3$ in the CAMx v7.0 replication run to 1.23 $\mu g/m^3$ in this test, compared to 2.51 $\mu g/m^3$ observed. NH_3 gas concentrations exhibited a minor reduction, which is consistent with additional SO_4 and particulate chloride, which were both neutralized by NH_4. Therefore, we speculate that the reduction in particle nitrate reflected a shift of NH_4 to the other acids, rather than any change in nitric acid production. In fact, small increases in Ox indicated that more oxidation did occur with higher HCl via nitryl chloride formation.

Figure 4-4 shows a time series of simulated $ClNO_2$ at Hawthorne for this test and the CAMx v7.0 replication run with reduced vertical mixing. Concentrations exceeded 1 ppb in the sensitivity case on some days and approached 1 ppb on several other days, which arguably may be the case in SLC given the availability of chloride emissions in the basin and the better agreement with particulate chloride measurements. The unmodified run resulted in $ClNO_2$ levels of a few tenths ppb, which are consistent with the urban plume results reported by Riedel et al. (2013) without the need for additional chloride.

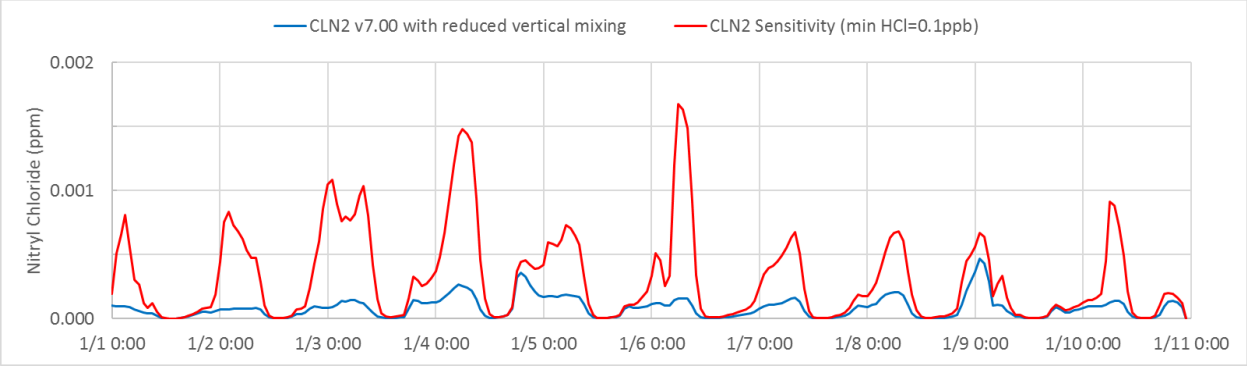

Figure 4-4. Time series of modeled hourly gas concentration of $ClNO_2$ at the Hawthorne monitoring site for the CAMx v7.0 replication run with reduced vertical mixing (blue) and the HCl sensitivity test (red) where background HCl concentration was set to 0.1 ppb.

Conclusion: Although artificially raising HCl levels improved particulate Cl performance, which is arguably appropriate, effects of enhanced chloride chemistry were minor for NOx and O_3 and had negligible effects on particle nitrate and total $PM_{2.5}$. Improvements in local chloride emission estimates and in modeling regional transport/dispersion patterns may improve the characterization of chlorides in the basin. The simple enhancement to background HCl was not continued into subsequent model tests.

4.3.3 Snow Albedo

The UDAQ snow modification described in Section 3 increased urban surface albedo to the range of 60-70%. In this test, we directly set snow-covered urban surface albedo to 80% (instead of

modifying snow cover fraction) to be more consistent with 2017 UWFPS albedo measurements and to boost photolysis rates. This change resulted in small (less than 1 $\mu g/m^3$) increases in ammonium nitrate and much smaller impacts on sulfate and organics. Increased photolysis rates shifted the NOx balance slightly (more daytime NO and less NO_2) and reduced daytime ozone.

Conclusion: The albedo increase had a minor effect, but we continued to include it for all remaining simulations as it is more consistent with observed albedo.

4.3.4 Effects of Clouds

As described in Section 3, UDAQ modified low-level clouds to reduce aqueous SO_4 production and related sulfate over predictions, with good success. However, clouds remain in the model and can reduce photolysis rates substantially. We conducted a rather artificial sensitivity test in which we completely removed all clouds from the simulation to maximize photolysis and further remove all aqueous SO_4 production. This resulted in a large reduction in $PM_{2.5}$ during the main inversion event (Janurary 7-8), especially at the Hawthorne monitoring site. SO_4 concentrations decreased by more than 1 $\mu g/m^3$ at several urban sites and on several days, with attendant NH_4 reductions, but there were only minor effects on particle nitrate (generally lower by less than 0.1 $\mu g/m^3$). Gaseous NH_3 concentrations were somewhat higher (consistent with lower NH_4) but there were no significant effects on NOx, O_3, or Ox. These results again indicate little particle nitrate sensitivity to the increased availability of NH_3 in the NO_3-limited conditions.

Conclusion: We found little photolysis sensitivity to the removal of clouds and an unwanted reduction in SO_4 and NH_4. The shift of NH_4 to NH_3 without moving to ammonium nitrate indicates NO_3-limited conditions where the environment is ammonia-saturated.

5.0 FINAL MODEL CONFIGURATION

Based on the sensitivity tests described in Section 4, we selected a final configuration of the model and its inputs that we believe results in the best overall improvements in simulating observed conditions during the January 2011 episode. As described in Section 3.2, the use of CAMx v7.0 leads to only negligible effects on organic and secondary inorganic $PM_{2.5}$ species concentrations, despite a major upgrade to organic PM chemistry (SOAP) and minor updates to inorganic and aqueous PM chemistry (ISORROPIA and RADM, respectively). On the other hand, we found large model sensitivity to a reduction in vertical diffusion rates and the replacement of UDAQ's NH_3 emission injection with a scale-up in on-road vehicle NH_3 emissions. We also found smaller sensitivity to an additional 40% scale-up of on-road vehicle NH_3 emissions for cold conditions and an increase in snow-covered urban albedo to 80%. All of these modifications are arguably appropriate and are supported by research in the scientific literature, and therefore we elected to include them in the final configuration. Table 5-1 lists the specific final model configuration and updates.

Table 5-1. The final CAMx v7.0 configuration for the SLC $PM_{2.5}$ modeling application, with UDAQ and Ramboll modifications noted (green text indicates no changes from the original UDAQ configuration, red indicates updates in v7.0 and those explicitly made in this project).

CAMx Process	V7.0 Model Configuration	Model/Input Modifications
Advection Solver	Piecewise Parabolic Method	
Gas-Phase Chemistry	Carbon Bond 6 revision 2, with full halogen chemistry (CB6r2h)	
Chemistry Solver	Euler Backward Iterative	
PM Chemistry	2-mode Coarse/Fine, ISORROPIA v1.7 inorganic chemistry (liquid-only metastable aerosols), RADM aqueous inorganic chemistry (updated metal-catalyzed and peroxide reactions), SOAP v2.2 organic chemistry	
Dry Deposition	Zhang (2001, 2003)	
Wet Deposition	Active	
Vertical Diffusion	Standard K-theory	Increased minimum vertical diffusion rates through 100 m
Surface Albedo		Set minimum urban snow cover albedo = 80%
Dry Deposition		Reduced NH_3 deposition by changing surface resistance from 0 (no resistance) to 1 (full resistance)
Dry Deposition		Set ozone deposition to zero
NH_3 Emissions		Replaced UDAQ NH_3 injection with scaled-up gasoline MV NH_3 emissions plus additional 40% increase for cold conditions.
Cloud Inputs		Reduced cloud water content of low-altitude clouds over Salt Lake County by 80%

Table 5-2 lists the episodic modeled emission inventory on the single day of January 7, 2011 for six Wasatch Front counties and for the entire 1.33 km modeling grid, aggregated to the four major source sectors. Note that the UDAQ county-specific NH_3 injection totals are listed under the area sector since it was treated as such. Ramboll's final vehicle NH_3 scale-up, which replaces the UDAQ injection, is listed under the on-road mobile sector. The UDAQ injection added 24 TPD over the six NAA counties (200% of the original total inventory), whereas the on-road scaling added only 4 TPD to six counties (34% of the original total inventory), which combined with reduced vertical mixing achieved similar or slightly better results for ammonium nitrate in the central SLC area.

Table 5-2. Modeled emission inventory (TPD) on January 7, 2011.

Sector	County	CO	NO_x	VOC	$PM_{2.5}$	SO_2	NH_3	NH_3 + Injection	NH_3 + Final Scaling
Area	Box Elder	1.0	0.6	2.5	0.2	0.01	1.9	11.5	--
	Davis	3.6	2.8	8.5	0.7	0.02	0.4	2.1	--
	Salt Lake	12.1	10.0	29.1	3.4	0.09	1.2	2.9	--
	Tooele	1.0	0.7	2.0	0.2	0.01	0.7	5.7	--
	Utah	7.5	4.4	12.5	1.5	0.05	3.4	7.3	--
	Weber	3.3	2.3	6.3	0.6	0.02	0.7	2.8	--
	1.33 km Grid	**35**	**23**	**69**	**7.9**	**0.3**	**13**	**52**	--
On-road	Box Elder	41.0	9.3	0.2	0.4	0.03	0.1	--	0.2
	Davis	95.9	18.2	0.5	1.0	0.09	0.4	--	0.9
	Salt Lake	347.2	59.9	1.6	3.5	0.34	1.3	--	3.4
	Tooele	32.7	8.2	0.2	0.4	0.02	0.1	--	0.2
	Utah	149.8	35.2	0.7	2.0	0.15	0.5	--	1.3
	Weber	65.7	11.2	0.3	0.6	0.07	0.2	--	0.7
	1.33 km Grid	**826**	**163**	**4**	**9**	**0.8**	**3**	--	**7**
Nonroad	Box Elder	2.8	1.4	0.2	0.05	0.01	0.001	--	--
	Davis	10.9	2.6	1.0	0.19	0.02	0.002	--	--
	Salt Lake	59.8	9.5	5.1	0.56	0.31	0.007	--	--
	Tooele	1.4	1.4	0.2	0.05	0.01	0.001	--	--
	Utah	18.9	3.1	1.8	0.23	0.02	0.003	--	--
	Weber	15.5	2.2	2.9	0.17	0.02	0.002	--	--
	1.33 km Grid	**138**	**24**	**20**	**1.6**	**0.4**	**0.02**	--	--
Point	Box Elder	2.6	1.0	0.6	0.5	0.1	0.01	--	--
	Davis	6.3	3.4	4.3	0.5	1.1	0.39	--	--
	Salt Lake	5.3	12.4	2.5	1.7	4.3	0.17	--	--
	Tooele	1.2	2.7	1.6	2.5	0.1	0.08	--	--
	Utah	0.6	1.2	0.6	0.3	0.1	0.24	--	--
	Weber	0.2	0.4	0.0	0.1	0.0	0.02	--	--
	1.33 km Grid	**20**	**26**	**10**	**5.9**	**6.8**	**1.0**	--	--
1.33 km Grid Grand Total		**1,018**	**236**	**104**	**24**	**8.3**	**17**	**56**	**21**

We ran CAMx v7.0 with the final configuration and reevaluated performance in replicating measured PM and gas concentrations during the January 1-11, 2011 modeling episode. We then applied the same emission modifications to UDAQ's projected inventories for the years 2017 and 2019 and re-ran CAMx for those projected emission scenarios. Results from those runs were used to project $PM_{2.5}$ concentrations to the 2019 attainment year to assess differences from UDAQ's projection. Details of the model performance evaluation and projections are presented below.

5.1 Model Performance Evaluation

Figure 5-1 compares modeled 24-hour $PM_{2.5}$ species concentrations against measurements at two sites, Hawthorne and Lindon, on January 7 when total $PM_{2.5}$ concentrations peaked during the episode. The figure shows results from the v7.0 replication run (repeated from Section 3.2 to facilitate comparison) and the final v7.0 run described above. Although the final run continued to under predict total $PM_{2.5}$ at these two sites, agreement for total $PM_{2.5}$ and most individual species improved markedly relative to the v7.0 replication run. In this case, the sum of elemental carbon (EC), OC and Other, which we can assume is nearly all associated with carbonaceous aerosol, tended to be over predicted at Hawthorne (22.6 $\mu g/m^3$ modeled vs. 15.3 $\mu g/m^3$ observed at Hawthorne) while well-predicted at Lindon (12.4 $\mu g/m^3$ modeled vs. 11.7 $\mu g/m^3$ observed at Lindon). We attribute this change from the v7.0 replication run to the reduction in vertical mixing. This suggests that primary

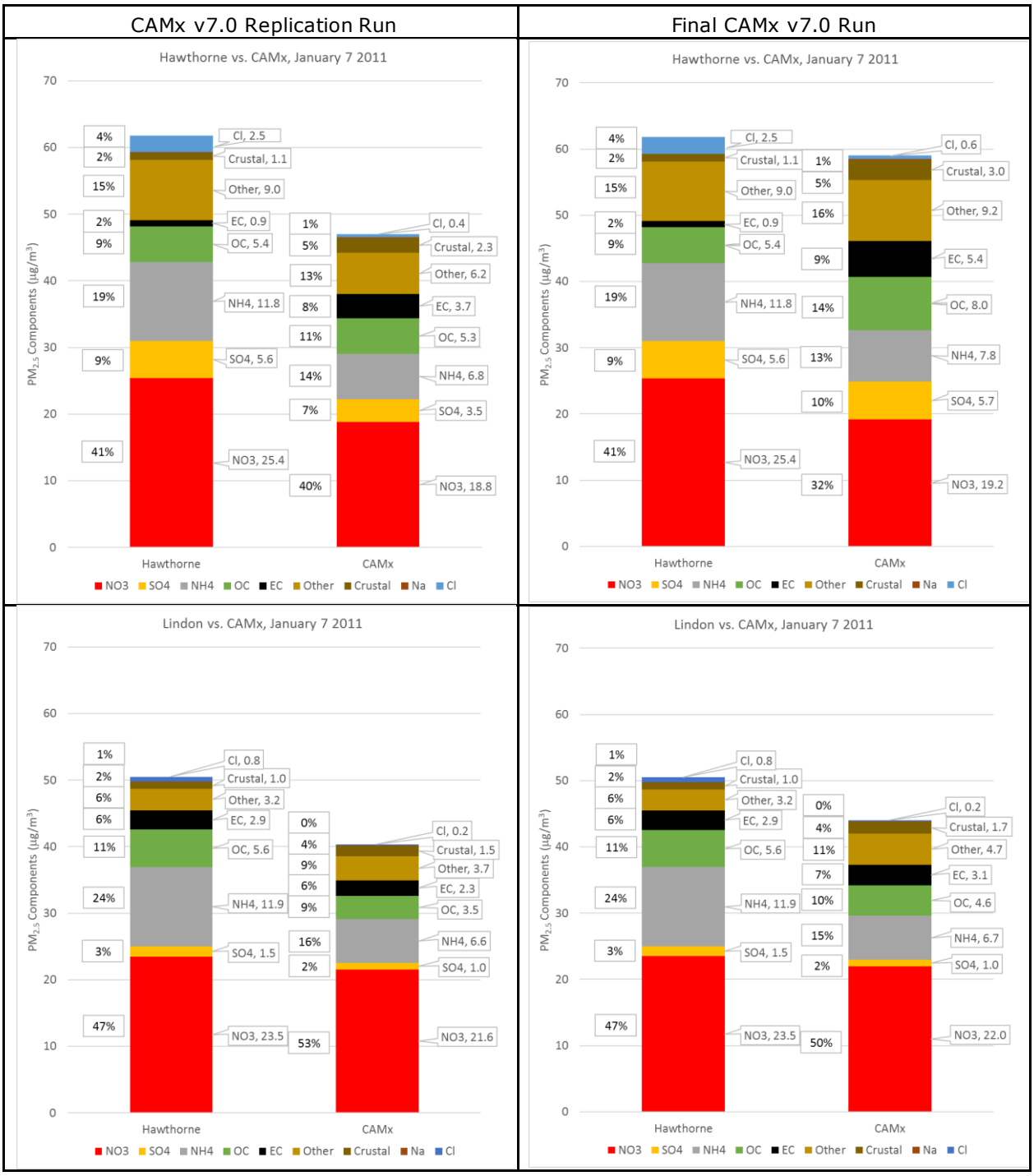

Figure 5-1. Comparison of modeled $PM_{2.5}$ species concentrations against measurements at Hawthorne (top) and Lindon (bottom) monitoring sites on January 7, 2011. Results from the v7.0 replication run are repeated at the left, results from the final v7.0 run are shown at the right. Boxed values to the right of each stacked bar indicate the absolute concentration ($\mu g/m^3$) and boxed values to the left indicate percent contribution to total $PM_{2.5}$.

carbon emissions from sources such as smoke may be over estimated in the SLC area and that the split among primary OC and EC emissions may need adjustment at the source-category level.

Table 5-3 lists statistical performance for individual 24-hour $PM_{2.5}$ species averaged over all three speciated monitoring sites and all 10 monitored site-days when measurements were available; compare to results from the v7.0 replication run in Table 3-2. Agreement improved for total $PM_{2.5}$ mass over all site-days, which resulted from improvements in organic and secondary inorganic compounds and relatively large increases (and related over predictions) in EC and crustal material. Again, certain species exhibited very large NMB and NME values, suggesting poor replication of measurements. However, the highest errors were associated with species that have small to negligible contributions to the $PM_{2.5}$ mass budget. When NMB is weighted by the measured relative contributions from each species in Table 5-4, the large errors in minor components are reduced substantially, revealing their actual insignificant contribution to overall $PM_{2.5}$ bias.

Figure 5-2 shows time series of modeled and measured total 24-hour $PM_{2.5}$ at six Federal Reference Method (FRM) monitoring sites in the Salt Lake and Utah Lake Basins. Table 5-5 presents $PM_{2.5}$ NMB and NME over the entire episode at each site and for the average over all sites for CAMx v7.0 replication and final runs. The model continued to capture the inter-daily variations. Total $PM_{2.5}$ concentrations at Hawthorne and Lindon improved over the CAMx v7.0 replication run but were similar to the replication run at other FRM sites.

Figure 5-3 shows time series of modeled and measured hourly gas concentrations at the Hawthorne monitoring site. Table 5-6 presents hourly gas NMB at the same site over the entire episode for both CAMx v7.0 final and replication runs. Results for all gases show consistent time variation with the v7.0 replication run, but with higher predicted concentrations for all but ozone, which is opposite. This is particularly evident in the CO and NH_3 time series, where the CO response was entirely caused by reduced vertical mixing whereas the NH_3 response was caused by a combination of reduced mixing and increased emissions. All gas species except for CO show improved episode-average statistical performance for bias relative to the v7.0 replication run. However, the time variations among all gases remained out of synch with measurements, which continued to indicate poor characterization of dispersion at hourly time scales. This may also be a cause for over predictions in primary carbon $PM_{2.5}$ emissions at Hawthorne during the middle of the episode.

Table 5-3. Statistical performance for speciated and total 24-hour $PM_{2.5}$ concentrations over all measured site-days of January 1-10, 2011 for the final CAMx v7.0 run. Statistical performance criteria from Emery et al. (2016) are also shown for context. Statistics within the criteria are displayed as green, those outside are displayed as red.

Species	NMB	NME	Criteria NMB	Criteria NME
NO_3	-35%	36%	<±65%	<115%
SO_4	2%	28%	<±30%	<50%
NH_4	-44%	47%	<±30%	<50%
OC	16%	44%	<±50%	<65%
EC	115%	119%	<±40%	<75%
Other	-30%	39%	N/A	N/A
Crustal	115%	125%	N/A	N/A
Na	151%	151%	N/A	N/A
Cl	-79%	79%	N/A	N/A
$PM_{2.5}$	-22%	28%	<±30%	<50%

Table 5-4. Mass-fraction weighted contribution of species NMB from Table 5-3 to total $PM_{2.5}$ NMB. Average mass fractions are determined from all measured site-days.

Species	% $PM_{2.5}$ Mass	Weighted NMB
NO_3	43%	-15%
SO_4	5%	0%
NH_4	18%	-8%
OC	10%	2%
EC	3%	4%
Other	17%	-5%
Crustal	2%	2%
Na	0%	0%
Cl	3%	-2%
$PM_{2.5}$	100%	-22%

Table 5-5. Statistical performance for total 24-hour $PM_{2.5}$ concentrations at FRM sites in the Salt Lake and Utah Lake Basins over January 1-10, 2011 for the initial CAMx v7.0 replication run and the final v7.0 run. Improvements are noted in green, declines are noted in red.

	NMB		NME	
FRM Site	V7.0 Replication	V7.0 Final	V7.0 Replication	V7.0 Final
Hawthorne	-31%	-16%	31%	25%
Lindon	-33%	-25%	33%	25%
Bountiful	-35%	-28%	35%	37%
Brigham City	-67%	-69%	67%	69%
Ogden	-42%	-39%	42%	40%
Tooele	-27%	-31%	27%	31%
All Sites	-37%	-30%	37%	34%

Table 5-6. Statistical performance for hourly gas concentrations at the Hawthorne monitoring site over January 1-10, 2011 for the initial CAMx v7.0 replication run and the final v7.0 run. Improvements are noted in green, declines are noted in red.

Gas Species	V7.0 Replication NMB	V7.0 Final NMB
Carbon Monoxide (CO)	1%	35%
Nitric Oxide (NO)	-50%	-9%
Nitrogen Dioxide (NO_2)	-30%	-16%
Nitrogen Oxides (NOx)	-40%	-12%
Ozone (O_3)	125%	86%
Odd Oxygen (Ox)	5%	1%

Figure 5-2. Time series of CAMx v7.0 replication run (blue), CAMx v7.0 final run (orange), and measured (black) total $PM_{2.5}$ at six FRM sites in the Salt Lake and Utah Lake Basins. The 24-hour $PM_{2.5}$ standard is shown as the horizontal red line.

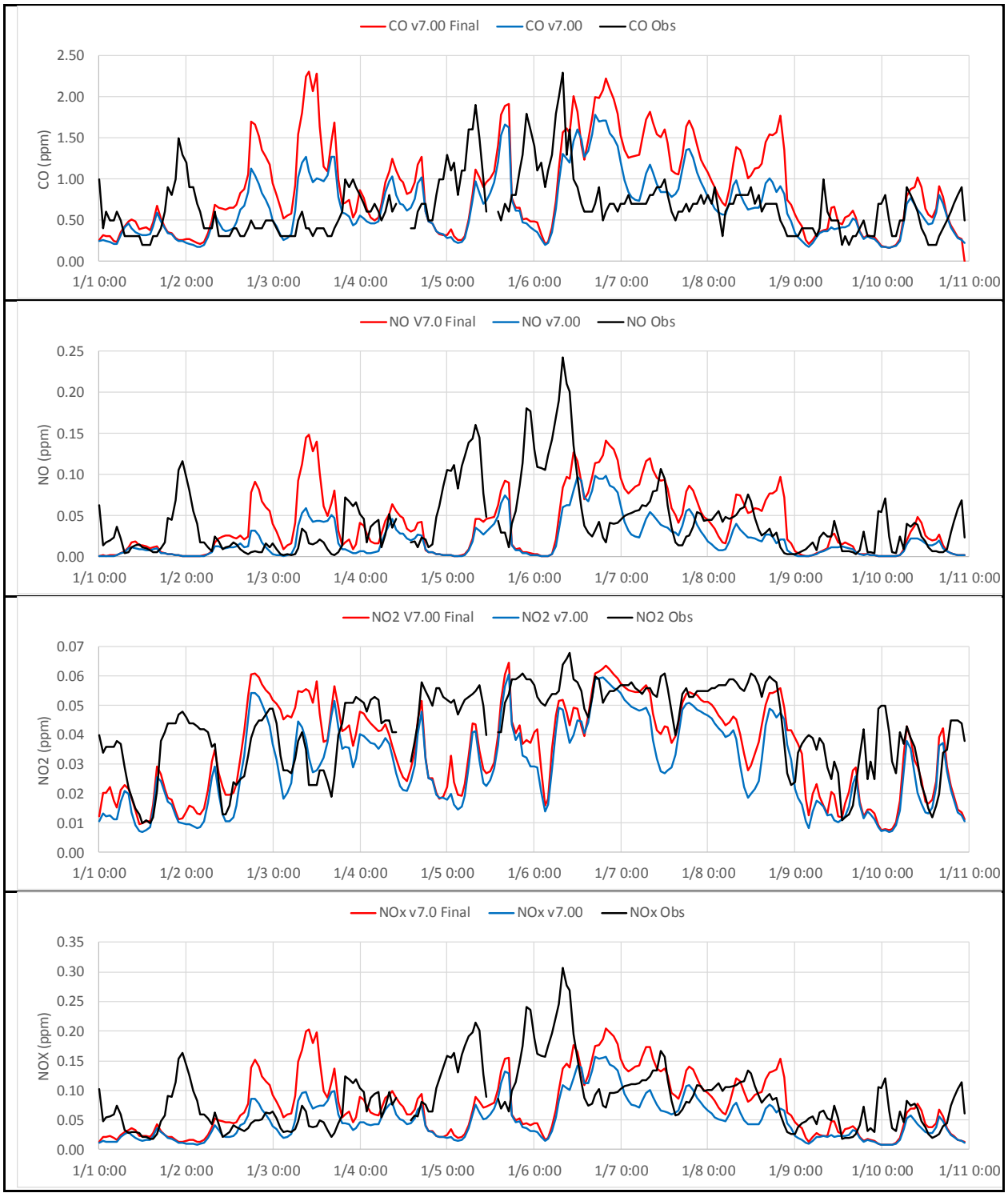

Figure 5-3. Time series of CAMx v7.0 replication run (blue), CAMx v7.0 final run (red), and measured (black) hourly gases at the Hawthorne monitoring site. Measurements of NH_3 are unavailable and modeled results are shown for context.

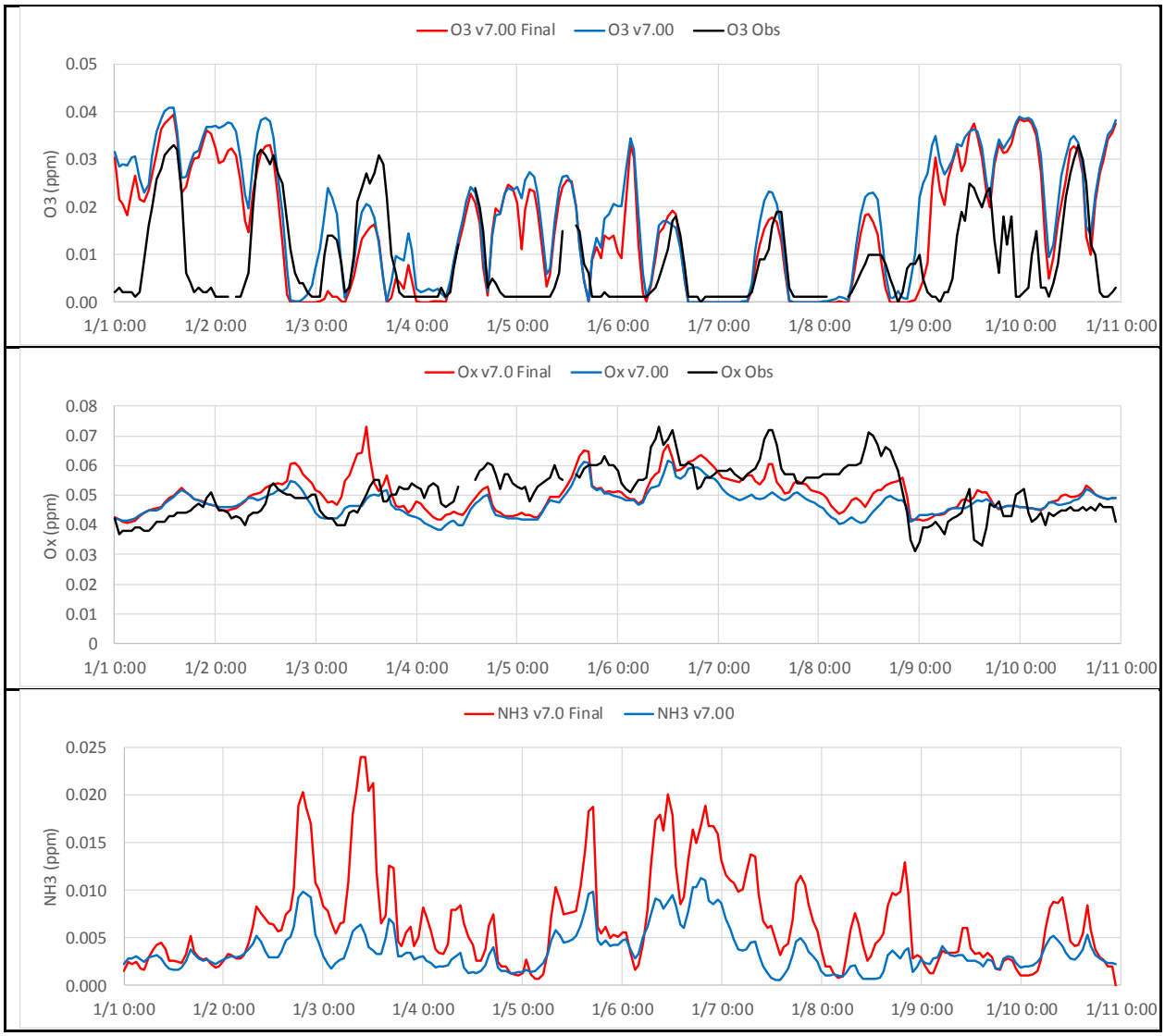

Figure 5-3 (concluded).

Simulated NH_3 concentrations ranged from a few ppb to well over 25 ppb on certain days of the episode (compared to a peak of 10 ppb in the v7.0 replication run), in much better qualitative agreement with measurements from the February 2019 WaFACO study. Figure 5-4 compares NH_3 concentration patterns averaged over February 2019 to modeled NH_3 concentrations averaged over January 3-8, 2011 from the final CAMx run. The model reproduced spatial patterns rather well throughout the Wasatch Front modeling domain and the concentration magnitudes approached measurements. In the Salt Lake Valley, maximum concentrations aligned with population density along the I-15 corridor and in central SLC, showing the dominance of on-road and commercial/industrial sources. The measured peak NH_3 in southwest Salt Lake County extending above 18 ppb is related to a landfill facility, which is not included in the model's emission inventory. Measured NH_3 patterns in Davis, Weber and Utah Counties indicate the dominance of agricultural emissions, where the model continued to under predict. This lack of NH_3 could explain much of the $PM_{2.5}$ under predictions at Ogden and Brigham City.

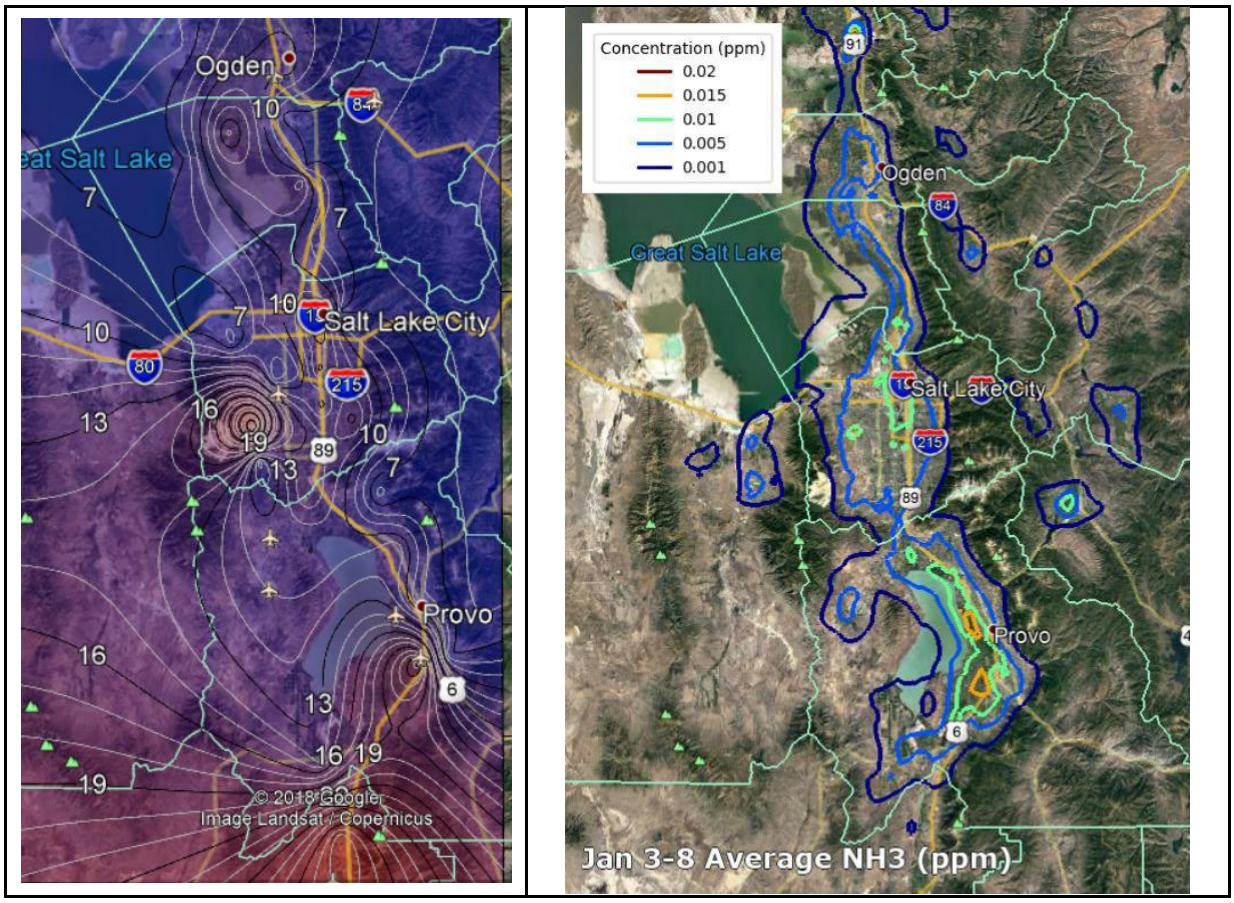

Figure 5-4. Left side shows the spatial distribution of measured NH_3 (ppb) averaged over the February 2019 WaFACO field study. Right side shows the spatial distribution of CAMx simulated NH_3 (ppm = ppb/1000) averaged over January 3-8, 2011 for the final CAMx run.

5.2 Design Value Projection

UDAQ provided 2017 and 2019 emission inventory files to Ramboll. We applied the same NH_3 emission modifications as described above to UDAQ's inventories and generated model-ready inputs to CAMx by running the inventory files through the SMOKE processing system in a manner consistent with UDAQ's configuration, speciation, and spatial/temporal definitions.

Diesel NH_3 was expected to contribute a larger fraction of total on-road emissions in years after the 2011 base case as SCR equipment required since 2007 (light-duty) and 2010 (heavy-duty) penetrated the diesel fleet. As shown in Table 5-7, UDAQ's MOVES run for 2019 does reflect increased NH_3 emissions from diesel vehicles and reduced NH_3 emissions from gasoline vehicles relative to 2011. We elected to apply the same 2011 gasoline vehicle NH_3 emissions scale-up by vehicle and roadway type to the 2017 and 2019 inventories as well. In fact, gasoline NH_3 emission factors reviewed in Appendix A were based on field data from more recent years, so our derived scaling factors are more applicable to the 2017 and 2019 years than 2011.

Recall that we did not adjust diesel NH_3 emissions in the 2011 inventory because that year was relatively recent to the federal diesel SCR requirements (so little time to penetrate into the fleet). We elected not to introduce scaling of diesel NH_3 emissions for the 2017 and 2019 years because there is evidence to suggest that MOVES correctly estimates NH_3 emissions from diesels with SCR. Most US

Table 5-7. Modeled NH_3 emission inventory (TPD) on January 7, 2011 for the five most populated Wasatch Front counties. Emissions are shown for the 2011 and 2019 years, split by diesel and gasoline vehicles to show separate future projections.

	Diesel		Gasoline		2011 to 2019	
County	**2019**	**2011**	**2019**	**2011**	**Diesel Change**	**Gasoline Change**
Box Elder	0.02	0.02	0.08	0.10	20%	-23%
Davis	0.03	0.02	0.22	0.35	26%	-38%
Salt Lake	0.09	0.06	0.80	1.27	48%	-37%
Utah	0.08	0.05	0.39	0.49	66%	-22%
Weber	0.02	0.01	0.15	0.24	76%	-37%
Total	**0.24**	**0.16**	**1.63**	**2.45**	**49%**	**-33%**

manufactures adhere to a European ammonia emission standard (<10 ppm) and based on rough estimates of exhaust flow, 10 ppm is in-line with MOVES estimates. Furthermore, diesels equipped with SCR either adjust the dosing or include NH_3 cleanup catalysts to limit ammonia slip.

Table 5-8 lists the projected 2017 episodic modeled emission inventory on the single day of January 7, 2011 similarly to the 2011 inventory listed in Table 5-2. Table 5-9 shows the percent changes from the 2011 values. Tables 5-10 and 5-11 list the 2019 inventory and percent changes from 2011, respectively.

Table 5-8. Projected 2017 modeled emission inventory (TPD) on January 7, 2011.

Sector	County	CO	NO_x	VOC	$PM_{2.5}$	SO_2	NH_3	NH_3 + Injection	NH_3 + Final Scaling
Area	Box Elder	1.1	0.5	1.9	0.2	0.01	1.8	11.4	--
	Davis	3.8	2.2	8.4	0.8	0.02	0.5	2.1	--
	Salt Lake	12.6	8.5	27.3	3.1	0.13	1.3	3.0	--
	Tooele	1.2	0.7	1.3	0.2	0.01	0.7	5.7	--
	Utah	9.6	5.2	13.4	1.9	0.06	3.3	7.2	--
	Weber	3.5	1.8	6.0	0.6	0.02	0.7	2.8	--
	1.33 km Grid	**38**	**21**	**66**	**8**	**0.3**	**12**	**51**	--
On-road	Box Elder	16.4	3.8	0.1	0.1	0.0	0.06	--	0.1
	Davis	66.2	9.3	0.3	0.5	0.06	0.27	--	0.6
	Salt Lake	224.4	27.5	1.0	1.5	0.22	0.92	--	2.3
	Tooele	18.9	4.2	0.1	0.2	0.01	0.06	--	0.1
	Utah	113.5	18.1	0.5	1.0	0.11	0.51	--	1.1
	Weber	53.0	7.6	0.3	0.4	0.05	0.19	--	0.5
	1.33 km Grid	**544**	**85**	**2.5**	**4**	**0.5**	**2.2**	--	**5**
Nonroad	Box Elder	2.6	1.1	0.2	0.04	0.00	0.001	--	--
	Davis	12.8	2.6	1.0	0.15	0.01	0.004	--	--
	Salt Lake	75.8	11.5	5.6	0.61	0.33	0.012	--	--
	Tooele	2.2	1.2	0.1	0.04	0.00	0.001	--	--
	Utah	20.6	3.5	1.7	0.22	0.01	0.005	--	--
	Weber	14.8	2.5	2.1	0.15	0.01	0.003	--	--
	1.33 km Grid	**151**	**26**	**17**	**1.5**	**0.38**	**0.03**	--	--
Point	Box Elder	2.2	0.7	0.4	0.3	0.2	0.01	--	--
	Davis	2.9	2.1	4.1	0.2	0.3	0.08	--	--
	Salt Lake	5.5	13.9	2.4	3.1	3.2	0.24	--	--
	Tooele	0.9	2.9	1.8	1.7	0.0	0.01	--	--
	Utah	5.3	1.4	0.2	0.4	0.0	0.62	--	--
	Weber	0.3	0.2	0.1	0.2	0.0	0.00	--	--
	1.33 km Grid	**21**	**27**	**9**	**6**	**5**	**1.1**	--	--
1.33 km Grid Grand Total		**754**	**159**	**95**	**20**	**6.0**	**15**	**54**	**18**

Table 5-9. Relative change (percent) from 2011 to projected 2017 modeled emission inventory on January 7, 2011.

Sector	County	CO	NO_x	VOC	$PM_{2.5}$	SO_2	NH_3	NH_3 + Injection	NH_3 + Final Scaling
Area	Box Elder	14%	-11%	-23%	11%	33%	-5%	-1%	--
	Davis	6%	-21%	-1%	18%	-11%	6%	1%	--
	Salt Lake	5%	-15%	-6%	-9%	48%	8%	3%	--
	Tooele	21%	3%	-31%	5%	1%	0%	0%	--
	Utah	27%	19%	7%	23%	21%	-2%	-1%	--
	Weber	7%	-21%	-5%	1%	-11%	-2%	-1%	--
	1.33 km Grid	**9%**	**-9%**	**-5%**	**4%**	**-1%**	**-7%**	**-2%**	--
On-road	Box Elder	-60%	-59%	-67%	-70%	-48%	-35%	--	-35%
	Davis	-31%	-49%	-36%	-51%	-32%	-26%	--	-32%
	Salt Lake	-35%	-54%	-40%	-56%	-36%	-30%	--	-33%
	Tooele	-42%	-49%	-46%	-56%	-39%	-28%	--	-29%
	Utah	-24%	-49%	-30%	-51%	-26%	-6%	--	-13%
	Weber	-19%	-32%	-19%	-39%	-31%	-24%	--	-30%
	1.33 km Grid	**-34%**	**-48%**	**-38%**	**-52%**	**-33%**	**-24%**	--	**-28%**
Nonroad	Box Elder	-5%	-15%	-18%	-18%	-84%	38%	--	--
	Davis	18%	0%	2%	-22%	-46%	59%	--	--
	Salt Lake	27%	22%	11%	9%	7%	71%	--	--
	Tooele	50%	-14%	-24%	-16%	-75%	22%	--	--
	Utah	9%	14%	-4%	-2%	-52%	63%	--	--
	Weber	-4%	13%	-27%	-9%	-57%	33%	--	--
	1.33 km Grid	**10%**	**8%**	**-16%**	**-7%**	**-12%**	**48%**	--	--
Point	Box Elder	-14%	-23%	-38%	-41%	62%	18%	--	--
	Davis	-54%	-39%	-5%	-58%	-69%	-79%	--	--
	Salt Lake	3%	12%	-4%	77%	-25%	40%	--	--
	Tooele	-24%	8%	17%	-31%	-72%	-38%	--	--
	Utah	795%	17%	-61%	39%	-16%	157%	--	--
	Weber	54%	-40%	114%	83%	-90%	-22%	--	--
	1.33 km Grid	**8%**	**3%**	**-8%**	**4%**	**-30%**	**10%**	--	--
1.33 km Grid Grand Total		**-26%**	**-33%**	**-9%**	**-17%**	**-28%**	**-9%**	**-4%**	**-14%**

Table 5-10. Projected 2019 modeled emission inventory (TPD) on January 7, 2011.

Sector	County	CO	NO_x	VOC	$PM_{2.5}$	SO_2	NH_3	NH_3 + Injection	NH_3 + Final Scaling
Area	Box Elder	1.1	0.5	1.8	0.2	0.01	1.7	11.4	--
	Davis	3.7	1.9	8.1	0.8	0.02	0.5	2.1	--
	Salt Lake	12.6	7.4	26.2	3.1	0.13	1.3	3.0	--
	Tooele	1.2	0.7	1.4	0.2	0.01	0.7	5.7	--
	Utah	9.5	4.9	13.3	1.9	0.43	3.3	7.2	--
	Weber	3.5	1.6	5.7	0.6	0.02	0.7	2.8	--
	1.33 km Grid	**38**	**19**	**64**	**11**	**0.7**	**15**	**54**	--
On-road	Box Elder	19.0	4.6	0.09	0.2	0.02	0.08	--	0.2
	Davis	57.9	8.0	0.25	0.4	0.08	0.24	--	0.5
	Salt Lake	207.9	28.5	0.89	1.5	0.31	0.90	--	2.2
	Tooele	19.7	4.7	0.09	0.2	0.02	0.07	--	0.2
	Utah	90.9	19.3	0.39	1.0	0.16	0.47	--	1.1
	Weber	46.8	6.3	0.21	0.3	0.06	0.17	--	0.4
	1.33 km Grid	**492**	**87**	**2.2**	**4**	**0.7**	**2.2**	--	**5**
Nonroad	Box Elder	2.5	1.1	0.2	0.04	0.00	0.001	--	--
	Davis	12.2	2.4	0.9	0.16	0.01	0.004	--	--
	Salt Lake	72.1	8.9	5.4	0.53	0.28	0.012	--	--
	Tooele	2.5	1.2	0.2	0.04	0.01	0.001	--	--
	Utah	25.1	2.8	1.9	0.22	0.02	0.005	--	--
	Weber	13.7	1.9	1.8	0.13	0.01	0.003	--	--
	1.33 km Grid	**149**	**21**	**15**	**1.4**	**0.3**	**0.03**	--	--
Point	Box Elder	2.4	1.2	0.9	0.6	0.3	0.01	--	--
	Davis	4.2	2.4	3.1	0.2	0.6	0.09	--	--
	Salt Lake	7.5	20.1	2.3	3.2	3.0	0.38	--	--
	Tooele	0.9	3.2	2.1	2.5	0.0	0.01	--	--
	Utah	0.4	0.8	0.2	0.2	0.0	0.33	--	--
	Weber	0.3	0.5	0.2	0.2	0.0	0.01	--	--
	1.33 km Grid	**18**	**33**	**9**	**7**	**5**	**1.1**	--	--
1.33 km Grid Grand Total		**697**	**160**	**91**	**24**	**6.5**	**18**	**57**	**21**

Table 5-11. Relative change (percent) from 2011 to projected 2019 modeled emission inventory on January 7, 2011.

Sector	County	CO	NO_x	VOC	$PM_{2.5}$	SO_2	NH_3	NH_3 + Injection	NH_3 + Final Scaling
Area	Box Elder	13%	-19%	-27%	11%	30%	-7%	-1%	--
	Davis	4%	-32%	-5%	20%	-17%	7%	1%	--
	Salt Lake	4%	-26%	-10%	-8%	46%	10%	4%	--
	Tooele	20%	-6%	-29%	8%	1%	-1%	0%	--
	Utah	27%	13%	6%	26%	850%	-3%	-1%	--
	Weber	6%	-32%	-9%	2%	-15%	-3%	-1%	--
	1.33 km Grid	**11%**	**-19%**	**-7%**	**33%**	**120%**	**17%**	**4%**	--
On-road	Box Elder	-54%	-50%	-60%	-64%	-8%	-17%	--	-17%
	Davis	-40%	-56%	-45%	-59%	-13%	-35%	--	-39%
	Salt Lake	-40%	-52%	-46%	-57%	-9%	-32%	--	-35%
	Tooele	-40%	-43%	-47%	-51%	1%	-17%	--	-18%
	Utah	-39%	-45%	-47%	-48%	9%	-14%	--	-19%
	Weber	-29%	-44%	-33%	-49%	-12%	-31%	--	-38%
	1.33 km Grid	**-40%**	**-47%**	**-46%**	**-53%**	**-5%**	**-27%**	--	**-31%**
Nonroad	Box Elder	-8%	-20%	-20%	-25%	-87%	38%	--	--
	Davis	12%	-10%	-3%	-18%	-38%	73%	--	--
	Salt Lake	21%	-6%	5%	-5%	-8%	66%	--	--
	Tooele	71%	-13%	-1%	-18%	-18%	33%	--	--
	Utah	33%	-8%	7%	-5%	-15%	73%	--	--
	Weber	-11%	-12%	-38%	-23%	-52%	29%	--	--
	1.33 km Grid	**8%**	**-9%**	**-25%**	**-16%**	**-18%**	**48%**	--	--
Point	Box Elder	-7%	19%	48%	9%	97%	-13%	--	--
	Davis	-33%	-28%	-28%	-52%	-44%	-77%	--	--
	Salt Lake	40%	62%	-9%	84%	-30%	122%	--	--
	Tooele	-20%	15%	35%	1%	-57%	-17%	--	--
	Utah	-25%	-38%	-68%	-42%	-24%	38%	--	--
	Weber	84%	17%	422%	111%	14%	217%	--	--
	1.33 km Grid	**-8%**	**28%**	**-10%**	**26%**	**-31%**	**11%**	--	--
1.33 km Grid Grand Total		**-32%**	**-32%**	**-13%**	**-3%**	**-22%**	**9%**	**2%**	**0%**

We then re-ran CAMx with the 2017 and 2019 emission scenarios. We passed CAMx output fields to the EPA Speciated Model Attainment Test (SMAT) program to project $PM_{2.5}$ 2018 design values (DV) to 2019 (i.e., 2016-2018 DV period to 2017-2019 DV period). We also obtained UDAQ's CAMx output for 2017 and ran their unadjusted 2019 emission inventory with their NH_3 injection in the original UDAQ CAMx configuration (UDAQ had not run CAMx for their 2019 scenario). We passed UDAQ's output fields to SMAT to compare their 2019 projected DVs with our results. Table 5-12 presents results from UDAQ and Ramboll's SMAT projections for the 7 FRM $PM_{2.5}$ sites along the Wasatch Front that were active in 2016-2018. Note that a projected DV of ≥35.5 $\mu g/m^3$ exceeds the 24-hour $PM_{2.5}$ standard due to definition of the 35 NAAQS and associated rounding conventions. See also Appendix B for details of the SMAT calculations. Results among UDAQ and Ramboll SMAT projected DVs are very similar for this brief 2-year span with no sites projected to exceed the standard; as detailed in Appendix B, positive and negative projection factors occur among all $PM_{2.5}$ species and these differ among the UDAQ and Ramboll modeling results. Ramboll results indicate mostly small increases in inorganic secondary salts (NH_4, nitrate and sulfate) and small reductions in primary carbon species. UDAQ results indicate mostly small mixed changes among all species.

Table 5-12. 2016-2018 base year DV (DVb) and 2019 projected future DV (DVf) estimated using SMAT. The UDAQ projections used the original UDAQ CAMx configuration with 2017 and 2019 emissions as listed above and described in the Maintenance Plan (UDAQ, 2020a); Ramboll projections used the modified CAMx configuration with UDAQ's 2017 and 2019 emissions, without the UDAQ NH_3 injection, but with the on-road motor vehicle NH_3 scaling developed in this study.

AIRS ID	Site Name, County	2016-2018 DVb	UDAQ 2019 DVf	Ramboll 2019 DVf
490030003	Brigham City, Box Elder	32.4	33.5	33.4
490110004	Bountiful, Davis	28.5	28.3	28.6
490353006	Hawthorne, Salt Lake	33.4	34.0	33.2
490353010	Rose Park, Salt Lake	34.9	35.4	35.0
490494001	Lindon, Utah	31.1	29.8	30.6
490495010	Spanish Fork, Utah	28.4	28.9	28.5
490570002	Ogden, Weber	30.2	30.7	30.2

6.0 SUMMARY AND CONCLUSIONS

Ramboll investigated causes for an apparent NH_3 shortfall in the photochemical modeling application employed by UDAQ to support the recent SLC SIP and subsequent MP. This project also benefitted from the WaFACO field study conducted by USU during the winter of 2019. We reviewed NH_3 emission inventories and recently measured concentration patterns; investigated modeling uncertainties and deficiencies, updated the UDAQ model configuration and increased modeled NH_3 emissions from on-road vehicles according to peer-reviewed literature; and re-evaluated modeling results and projected attainment-year $PM_{2.5}$ air quality.

Based on comparisons to routine field measurements during the January 1-10, 2011 modeling episode, the UDAQ simulation replicated the relative contributions of most $PM_{2.5}$ species rather well but under predicted total $PM_{2.5}$ at all sites throughout the episode because of a lack of particulate ammonium nitrate, despite the additional NH_3 emissions. The simulated meteorology generally captured the build-up and cessation of the stagnant inversion pattern over the episode. However, comparison of observed and predicted concentrations of emitted gases (CO and NOx), which depend on different emission inventory sectors than ammonia, indicated that simulated meteorology did not sufficiently characterize inversion depth/strength, dispersion patterns or the degree of stagnation in time and space. We found that on average NOx was under predicted by about 20% during the episode while ozone was consistently over predicted (i.e., perhaps too little ozone uptake into NOx and its oxidation products rather than too much ozone formation). During mid-episode when $PM_{2.5}$ peaked, odd oxygen ($Ox = NO_2 + O_3$; a measure of photochemical processing among NOx and O_3) was under predicted, establishing a link relating low rates of NOx oxidation and the lack of nitrate production. Additionally, we found that even with UDAQ's additional NH_3, simulated NH_3 concentrations over the basin remained roughly a third of the average 11-12 ppb measured in SLC during the February 2019 WaFACO study.

The modeling system was rather sensitive to vertical diffusion rates:

On the basis of CAMx sensitivity testing, we found that simulated $PM_{2.5}$ and most gas concentrations benefitted greatly from reduced vertical mixing, which also reduced the apparent NH_3 shortfall, and likewise benefited somewhat from increased snow albedo, which enhances photochemical production of secondary species including nitrate.

The modeling system was insensitive to chemical modifications and bi-directional ammonia exchange with the snow-covered surface:

The model was insensitive to the introduction of bi-directional NH_3 surface exchange because the presence of snow cover squelches NH_3 re-emission from soil/vegetation. Additionally, snow enhances NH_3 deposition rates when snow partially melts during the daytime. The model was also insensitive to chemical modifications such as invoking alternative inorganic aerosol chemistry, removal of clouds (maximized solar radiation), increased chloride levels (increased oxidant production), and a scale-up of NOx emissions to alleviate the episode-average NOx under prediction bias.

Simulated $PM_{2.5}$ concentrations in urban SLC responded greatly to increased NH_3 emissions from on-road gasoline vehicles:

Simulated NH_3 and ammonium nitrate concentrations responded most favorably when we replaced the UDAQ NH_3 injection with a scale-up of on-road vehicle NH_3 emissions by a factor of ~2, a modification that is supported by the scientific literature. While the UDAQ NH_3 injection added ~65% to the

original total Salt Lake County episodic emission inventory, the on-road NH_3 scale-up added ~40%. Although we found major uncertainties in other NH_3 emission sectors, specifically animal husbandry and landfill/composting facilities, we did not alter those NH_3 emissions because of a lack of information needed to address fundamental issues with emission factors (emission rates per activity unit), a lack in estimated activity (animal head counts, composting volumes) and the manner in which these sources are spatially allocated to the modeling grid (to general widespread landuse categories rather than to specific locations/facilities). In the more rural counties of Box Elder, Weber, Tooele, and Utah under estimates of agricultural NH_3 are likely to be the primary cause for $PM_{2.5}$ under predictions.

Combining several key improvements, the final model resulted in improved agreement between measured and simulated $PM_{2.5}$ concentrations in SLC and Utah County:

We conducted a final CAMx base-year simulation for the episode, applying reduced vertical diffusion rates, increased urban snow albedo, and scaled-up on-road vehicle NH_3 emissions in lieu of the UDAQ NH_3 injection. While the model continued to under predict total $PM_{2.5}$, particularly at rural monitoring sites, agreement with speciated $PM_{2.5}$ measurements improved markedly at the urban monitoring sites relative to our initial CAMx replication run. The final model configuration predicted about the right amount of particulate sulfate and approached the 2019 episode-averaged measured concentrations of NH_3 in the SLC basin. However, the model continued to under estimate particulate nitrate by over 30%, averaged over all three speciated monitoring sites and monitored days, which is consistent with and generally better than other $PM_{2.5}$ modeling applications in the western US. This case also revealed that carbon emissions from sources such as smoke may be over estimated in the SLC area and that the split among primary organic and elemental carbon emissions may need adjustment at the source-category level.

Projected $PM_{2.5}$ Design Values using the updated model were similar to UDAQ's projections:

Finally, we conducted simulations using UDAQ's 2017 and 2019 projected emission inventories, applying the on-road vehicle NH_3 scale-up at the same proportion as 2011, and holding the model configuration and all other model inputs the same as the final base-year simulation described above. Results among UDAQ and Ramboll projected $PM_{2.5}$ DVs from 2016-2018 monitored DVs were very similar with no sites projected to exceed the standard. We confirmed that both our and UDAQ's projected cases do result in some small concentration increases for inorganic secondary salts (NH_4, nitrate and sulfate), indicating disbenefit conditions.

The model indicates the SLC basin exists in a NOx-disbenefit condition during PCAP events, in agreement with recent field studies:

Both modeled and measured ozone and NOx indicate that the gas-phase chemical environment that generates secondary $PM_{2.5}$ compounds during exceedance events is NOx-saturated and oxidant-lean. This is a separate issue from whether $PM_{2.5}$ formation is ammonia- vs. nitrate-limited. In a NOx-saturated environment, NOx emission reductions can raise oxidant levels, raise secondary PM formation rates, and cause $PM_{2.5}$ increases or smaller-than-expected decreases ("NOx dis-benefit"). Recent field studies and previous UDAQ analyses indicate the SLC atmosphere is typically in this regime during PCAP events and the behavior of the model is consistent with this. This has major implications for accurately projecting future $PM_{2.5}$ based on anticipated emission inventory changes.

The model indicates the SLC basin is near balance between ammonia-limited and nitrate-limited conditions, in agreement with recent field studies:

Our results provide ample evidence to suggest that the inorganic $PM_{2.5}$ environment in Salt Lake City can vary spatially and temporally between NH_3-limited and NO_3-limited conditions. The model is therefore responding appropriately to emission reductions with small reductions or increases in $PM_{2.5}$. However, the degree of $PM_{2.5}$ response is affected by model uncertainties and could change substantially if the particulate nitrate under prediction bias could be alleviated, thereby altering the balance between cations (NH_3) and acids (nitrate, SO_4, Cl).

Remaining Issues:

Remaining model performance issues are related to the ability of the meteorological model to properly represent weak flow patterns under stagnant inversion conditions, and remaining issues for certain stationary emission sectors, including activity, spatial distribution, temporal allocation, and speciation including the split of primary $PM_{2.5}$ emissions into specific carbon and non-carbon components.

6.1 Recommendations

Based on results from this study, we recommend the following for future research and modeling applications:

- Continue to employ the updates developed in this project for future $PM_{2.5}$ modeling analyses, including reduced vertical diffusion rates, increased on-road NH_3 emissions from gasoline vehicles, and increased snow-covered urban albedo;
- Bring the modeling system forward to a more recent exceedance episode to characterize contemporary $PM_{2.5}$ air quality along the Wasatch Front and to update future year projections;
- Investigate ways to improve the meteorological simulation of PCAP episode along the Wasatch Front, specifically in characterizing inversion depth and strength, three-dimensional dispersion patterns, and boundary layer cloud evolution;
- Improve NH_3 emission inventory and spatial allocation techniques for remaining key sources: livestock agriculture (particularly in more rural counties) and landfill/composting activities;
- Investigate causes for under estimates of NOx and chloride emissions;
- Research and implement alternative speciation profiles for wood combustion among organic and elemental carbon and non-carbon smoke components;
- Investigate how the collection of further model updates alter $PM_{2.5}$ response to future projected and/or alternative emissions scenarios;
- Further investigate the role of snow in modulating surface-atmosphere NH_3 exchange;

6.2 Data Sharing

The Ramboll team has shared with UDAQ all datasets and models developed or updated during the course of this project. Following the specifications in the Science for Solutions Grant, all shared data was provided to UDAQ within 8 months of project completion. The following data were delivered to UDAQ from this project:

- The updated CAMx modeling system, including all CAMx source code updates specific to this work, model scripts, input and output files (all other general CAMx updates are periodically made available to the public at Ramboll's website www.camx.com);

- All emissions inventory and model-ready emission files that Ramboll adjusted or altered, including scaled-up on-road vehicle NH_3 emissions as SMOKE-ready inputs, CAMx-ready inputs, and tabular spreadsheet summaries;
- All other adjusted or altered model inputs, specifically the modified vertical diffusion input files;
- A subset of key CAMx output files selected in coordination with UDAQ, both for the 2011 performance evaluation period and the 2017-2019 projection scenarios.

7.0 REFERENCES

Baasandorj, M., et al., 2018. "2017 Utah Winter Fine Particulate Study Final Report." Prepared for the Utah Division of Air Quality (UDAQ), March 16, 2018. https://documents.deq.utah.gov/air-quality/planning/technical-analysis/research/northern-utah-airpollution/utah-winter-fine-particulate-study/DAQ-2018-004037.pdf.

CMAS, 2019. SMOKE v3.6.5 User's Manual. Prepared by the Community Modeling and Analysis System, University of North Carolina, Institute for the Environment. Available at: https://www.cmascenter.org/smoke/documentation/3.6.5/html/.

Crossman, E., C. Foster, 2016. PM2.5 State Implementation Plan: Meteorological Modeling. Prepared by the University of Utah, Department of Atmospheric Sciences, for the Utah Division of Air Quality (16 November, 2016).

Durbina, T.D., et al., 2004. The effect of fuel sulfur on NH3 and other emissions from 2000–2001 model year vehicles. *Atmospheric Environment*, 38, 2699–2708.

Emery, C., Z. Liu, A.G. Russell, M.T. Odman, G. Yarwood, N. Kumar, 2016. Recommendations on statistics and benchmarks to assess photochemical model performance. *Journal of the Air & Waste Management Association*, http://dx.doi.org/10.1080/10962247.2016.1265027.

EPA, 2019a. Clean Data Determination; Salt Lake City, Utah 2006 Fine Particulate Matter Standards Nonattainment Area. Federal Register, Vol. 84, No. 188 (September 27, 2019; EPA–R08–OAR–2019–0081; FRL–9999–66–Region 8). https://www.govinfo.gov/content/pkg/FR-2019-09-27/pdf/2019-20380.pdf#page=1.

EPA, 2019b. MOtor Vehicle Emission Simulator (MOVES) website: https://www.epa.gov/moves.

Helmig, D., C. Stephens, J.-H. Park, J. Hueber, P. Boylan, J. Evans, 2014. Ozone Deposition Velocity During Snow-Covered and Non-Snowcovered Periods by Eddy Covariance. Institute of Arctic and Alpine Research, University of Colorado Boulder (March, 2014). https://documents.deq.utah.gov/air-quality/technical-analysis/DAQ-2017-009834.pdf

Huai, T., T.D. Durbin, J.W. Miller, J.T. Pisano, C.G. Sauer, S.H. Rhee, J.M. Norbeck, 2003. "Investigation of the Formation of NH3 Emissions as a Function of Vehicle Load and Operating Condition." Presented at the 12th Annual Emission Inventory Conference, San Diego, CA, USA.

Metzger, S., B. Steil, M. Abdelkader, K. Klingmüller, L. Xu, J.E. Penner, C. Fountoukis, A. Nenes, J. Lelieveld, 2016. Aerosol water parameterisation: a single parameter framework. *Atmos. Chem. Phys.*, 16, 7213-7237.

Nenes, A, C. Pilinis, S.N. Pandis, 1998. ISORROPIA: A New Thermodynamic Model for Multiphase Multicomponent Inorganic Aerosols. *Aquatic Geochemistry*, 4, 123-152.

Nenes, A., C. Pilinis, S.N. Pandis, 1999. Continued Development and Testing of a New Thermodynamic Aerosol Module for Urban and Regional Air Quality Models. *Atmos. Environ.*, 33, 1553-1560.

Ramboll, 2020. Comprehensive Air quality Model with extensions, www.camx.com.

Riedel, T.P., et al., 2013. Chlorine activation within urban or power plant plumes: Vertically resolved $ClNO_2$ and Cl_2 measurements from a tall tower in a polluted continental setting. *J. Geophys. Res. Atmos.*, 118, 8702–8715, doi:10.1002/jgrd.50637.

Skamarock, W.C., J.B. Klemp, J. Dudhia, D.O. Gill, D. Barker, M.G. Duda, … J.G. Powers, 2008. A Description of the Advanced Research WRF Version 3 (No. NCAR/TN-475+STR). University Corporation for Atmospheric Research, doi:10.5065/D68S4MVH.

Suarez-Bertoa, R., A.A. Zardini, C. Astorga, 2014. Ammonia exhaust emissions from spark ignition vehicles over the New European Driving Cycle. *Atmospheric Environment*, 97, 43-53.

Sun, K., L. Tao, D.J. Miller, M.A. Khan, M.A. Zondlo, 2014. On-Road Ammonia Emissions Characterized by Mobile, Open-Path Measurements. *Environ. Sci. Technol*., 48, 3943−3950. https://pubs.acs.org/doi/abs/10.1021/es4047704.

Sun, K., L. Tao, D.J. Miller, D. Pan, L.M. Golston, M.A. Zondlo, R.J. Griffin, H.W. Wallace, Y.J. Leong, M.Y.M. Yang, Y. Zhang, D.L. Mauzerall, T. Zhu, 2016. Vehicle Emissions as an Important Urban Ammonia Source in the United States and China. *Environ. Sci. Technol.*, DOI:10.1021/acs.est.6b02805.

UDAQ, 2018. "Utah State Implementation Plan: Control Measures for Area and Point Sources, Fine Particulate Matter, Serious Area PM2.5 SIP for the Salt Lake City, UT Nonattainment Area (Section IX. Part A.31)." December 5, 2018. https://documents.deq.utah.gov/air-quality/pm25-serious-sip/DAQ-2018-013088.pdf.

UDAQ, 2020a. PM2.5 Salt Lake City Maintenance Plans: Technical Support Documents. https://deq.utah.gov/air-quality/pm2-5-salt-lake-city-maintenance-plans-technical-support-documents.

UDAQ, 2020b. Wasatch Front Ammonia and Chloride Observations (WaFACO). https://deq.utah.gov/air-quality/wasatch-front-ammonia-and-chloride-observations-wafaco.

Wentworth, G.R., J.G. Murphy, K.B. Benedict, E.J. Bangs, J.L. Collett, 2016. The role of dew as a night-time reservoir and morning source for atmospheric ammonia. *Atmos. Chem. Phys.*, 16, 7435–7449. www.atmos-chem-phys.net/16/7435/2016/doi:10.5194/acp-16-7435-2016.

Whaley, C.H., Makar, P.A., Shephard, M.W., Zhang, L., Zhang, J., Zheng, Q., Akingunola, A., Wentworth, G.R., Murphy, J.G., Kharol, S.K., Cady-Pereira, K.E., 2018. Contributions of natural and anthropogenic sources to ambient ammonia in the Athabasca Oil Sands and north-western Canada. *Atmos. Chem. Phys*., 18(3), 2011-2034.

Zhang, L., Brook, J.R., Vet, R., 2003. A revised parameterization for gaseous dry deposition in air-quality models. *Atmos. Chem. Phys*., 3(6), 2067-2082.

Zhang, L., Wright, L.P., Asman, W.A.H., 2010. Bi-directional air-surface exchange of atmospheric ammonia: A review of measurements and a development of a big-leaf model for applications in regional-scale air-quality models. *J. Geophys. Res.: Atmos*., 115(D20).

APPENDIX A: REVIEW OF MOBILE SOURCE AMMONIA EMISSIONS MEASUREMENTS

A.1 Introduction

Ammonia (NH_3) emissions from engines are primarily the result of aftertreatment catalysts to reduce nitrogen oxide (NOx) emissions. In gasoline or natural gas spark-ignition engines, the formation of NH_3 occurs through the chemical reduction of nitric oxide (NO) in a three-way catalyst (TWC). In such cases, NH_3 and nitrous oxide (N_2O) are intermediate products of the chemical reduction of NO, the primary form of NOx from an engine. Hydrogen (H_2) is used as the reductant, formed through a water (H_2O)-gas shift reaction from methane (CH_4) and carbon monoxide (CO). The presence of H_2 and CO can also form NH_3 as outlined the following chemical reactions:

$$CH_4 + H_2O \rightarrow CO + 3H_2$$
$$CO + H_2O \rightarrow CO_2 + H_2$$
$$2NO + 4CO + 2H_2O + H_2 \rightarrow 2NH_3 + 4CO_2$$
$$2NO + 5H_2 \rightarrow 2NH_3 + 2H_2O$$

As presented by (Nevalainen et al. 2018), Figure A-1 demonstrates that NH_3 is formed when the exhaust concentrations are near stoichiometric air-fuel ratios where most modern spark-ignition engines operate.

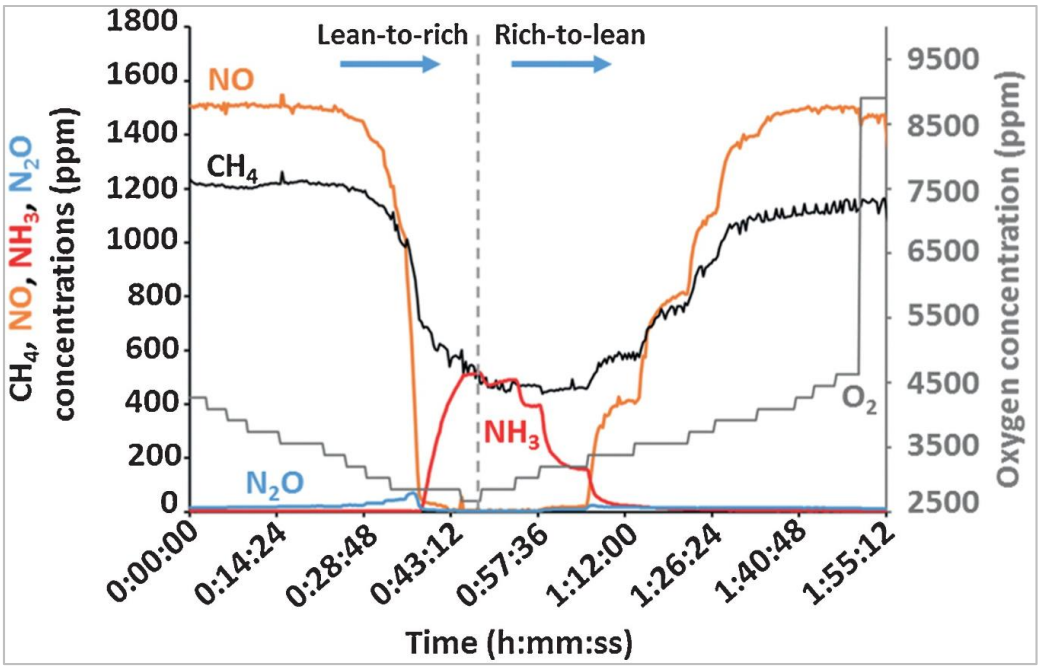

Figure A-1. CH_4, NO, NH_3 and N_2O concentrations during lean-to-rich and rich-to-lean operations and oxygen concentration at 440 °C with fresh TWC (Nevalainen et al. 2018).

In modern compression-ignition engines (primarily diesel or diesel pilot injection) where the air-fuel mixture is lean, Selective Catalytic Reduction (SCR) is used to reduce NO emissions. NH_3 is added upstream of the SCR typically by injecting urea solution that thermally decomposes to NH_3. This raises the possibility for NH_3 emissions if it "slips" through the catalyst without reacting. However, modern diesel engines usually include an NH_3 oxidation (AMOX) catalyst to minimize slip into the atmosphere, but this may not eliminate all NH_3 emissions. If the aftertreatment controls begin to fail,

NH_3 emissions are possible. Since model year 2010, heavy-duty diesel engines are required to have NOx controls that encourage the use of SCR. Likewise, the 2007 light-duty vehicle standards necessitate aftertreatment NOx control. The use of SCR for off-road diesel engines was phased in during 2014-2017 to meet the Tier 4 emissions standards.

A.2 Ambient Tunnel and Remote Sensing Measurements

Ambient NH_3 emission measurements include remote sensing studies both in tunnels and of individual vehicles. In both cases, it is difficult to relate the NH_3 concentration to actual emissions rates in terms of vehicle miles traveled, so the measured and reported NH_3 concentrations are expressed relative to carbon dioxide (CO_2) concentration (over ambient). These are converted to mass of emissions (g) per mass of fuel consumed (kg) using a carbon balance. Tunnel studies represent fleet averages incorporating the age distribution of the fleet passing through the tunnel, while remote sensing measures individual vehicles and matches the license plate to the make, model, and year through the vehicle registration.

A.2.1 Light-Duty Gasoline Vehicles

Because only a small fraction of light-duty vehicles is diesel powered, field studies largely measured the fleet of gasoline light-duty vehicles. Heavy-duty vehicles are not measured during most remote sensing studies because of the location of exhaust pipes or because they were specifically excluded based on the vehicle registration.

Sun et al. (2016) provided a summary of the findings from tunnel and remote sensing field study reports produced through 2016. Results ranged from 0.27 to 0.66 (ppb NH_3 / ppm CO_2). The estimates from the US field studies (including Tulsa, Houston, Philadelphia, and cities in California) since 2013 averaged 0.37 ppb/ppm, and that result translates to an NH_3 emission rate of 0.45 g/kg-fuel. Another tunnel study (Kean et al., 2009) in the San Francisco Bay area also found that NH_3 emissions from a fleet of light-duty vehicles were 0.64±0.04 g/kg-fuel in 1999 and 0.40±0.02 mg/kg-fuel in 2006.

The average result from historic studies is within the range of recent measurements in Los Angeles by Bishop (2019), which range from 0.62 g/kg-fuel to 0.43 g/kg-fuel. In that study, results from two measurement sites differed in that the higher NH_3 emissions were produced at the site where traffic travels along an arterial roadway with traffic light controls forcing stop and go driving, while lower NH_3 emissions were produced at the site where traffic travels on a limited access road (freeway) without traffic light controls. Bishop's (2019) results were also parsed by vehicle model year (Figure A-2), where aged vehicles produced higher NH_3 emissions compared with newer vehicles (by about a factor of 3 for 20-24 year-old vehicles). Note that NH_3 is produced only when the catalyst is actively reducing NOx emissions, so even aged catalysts function effectively to reduce NOx while producing more NH_3.

A.2.2 Heavy-Duty Diesel Vehicles

Haugen et al. (2018) remotely measured NH_3 emissions at a weigh station in California and found 0.09 g/kg-fuel in 2017 for the 1844 heavy-duty vehicles measured, 0.02 g/kg-fuel in 2012, and 0.003 g/kg-fuel in 2009. The big difference between the three years is that 63% of the heavy-duty diesel fleet in 2017 comprised chassis model years 2011+ (with 2010 and later engines) compared to only 12% in 2012, and 0% in 2009. Therefore, NH_3 emissions largely occur when the SCR catalysts are used on modern vehicles. Based on this information, we would expect that modern heavy-duty diesel vehicles (if 100% of the vehicles were 2011+) would produce 0.14 g/kg-fuel.

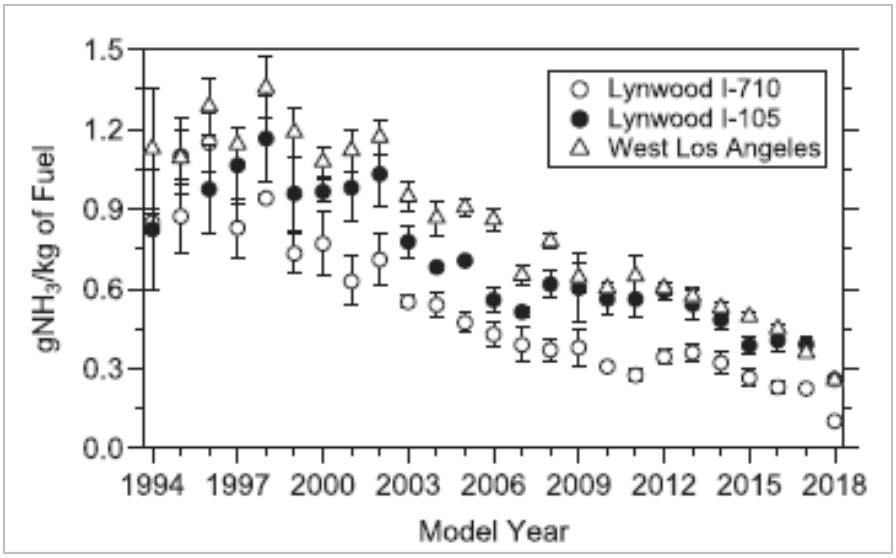

Figure A-2. NH_3 emissions by vehicle age at three remote sensing sites in Los Angeles, California. Uncertainties are represented by standard error of the mean calculated using daily means (Bishop, 2019).

A.3 Individual Vehicle Emissions Measurements

Vehicle emissions measurements come from two types, laboratory studies on prescribed driving cycles and portable emission monitoring systems (PEMS) used for normal driving on the road. Laboratory studies require that the vehicle is loaded by a dynamometer that provides resistance to the wheels of a vehicle or the fly wheel of the engine, and emissions are measured in accordance to standard certification conditions. The laboratory conditions can be controlled and replicated from test to test and vehicle to vehicle. Laboratory studies can be unrepresentative of normal operations including road roughness, route turns, ambient weather and other conditions. PEMS devices can be used whenever the vehicle is operated and can be conducted in a laboratory or on the road to compare the situations. However, PEMS devices add significant weight and can change the vehicle dynamics and may not conform to the certification measurement methods.

A.3.1 Light-Duty Gasoline Vehicles

Laboratory studies often use certification cycles or other driving cycles meant to represent in-use conditions. Many typical cycles that are used for certification include the U.S. Federal Test Procedure (FTP), the European New European Driving Cycle (NEDC), and the Worldwide Harmonized Light Vehicles Test Cycle (WLTC). In these cycles, the vehicles are required to be started and so can include cold and hot starts separately or combined. Other cycles can be driven in a laboratory, but it might not be possible to accurately represent in-use conditions of road roughness, grade, and other variables.

Suarez-Bertoa et al (2017) provides a summary of some historic studies of NH_3 emissions from light-duty gasoline US and European vehicles, indicating 3 to 48 mg/km (5 – 77 mg/mi) on typical certification driving cycles. Suarez-Bertoa et al. (2014) report that the range of NH_3 emissions from Euro V and Euro VI vehicles was 4 to 62 mg/km with one diesel vehicle at ~8 mg/km.

In addition, Suarez-Bertoa et al. (2014, 2017) report that cold conditions and cold starts result in higher NH_3 emissions for gasoline vehicles (by 28% to 47%, respectively, among the two papers). In Suarez-Bertoa et al. (2017), cold starts were responsible for up to 134 mg/km NH_3 of each trip

measured, where the length of the cold start period was determined by engine temperature, but no longer than 5 minutes, so the travel distance was likely less than 1 km. However, the overall average for the gasoline vehicle NH_3 emission factor based on hot start trips averaged 6±2 mg/km, so the vehicles used for the cold testing conditions were normally low NH_3 emitters. One reason given by Suarez-Bertoa et al. (2017) for the higher NH_3 emissions relates to higher CO emissions, and Figure A-3 shows that cold temperatures have an effect regardless of the CO emissions.

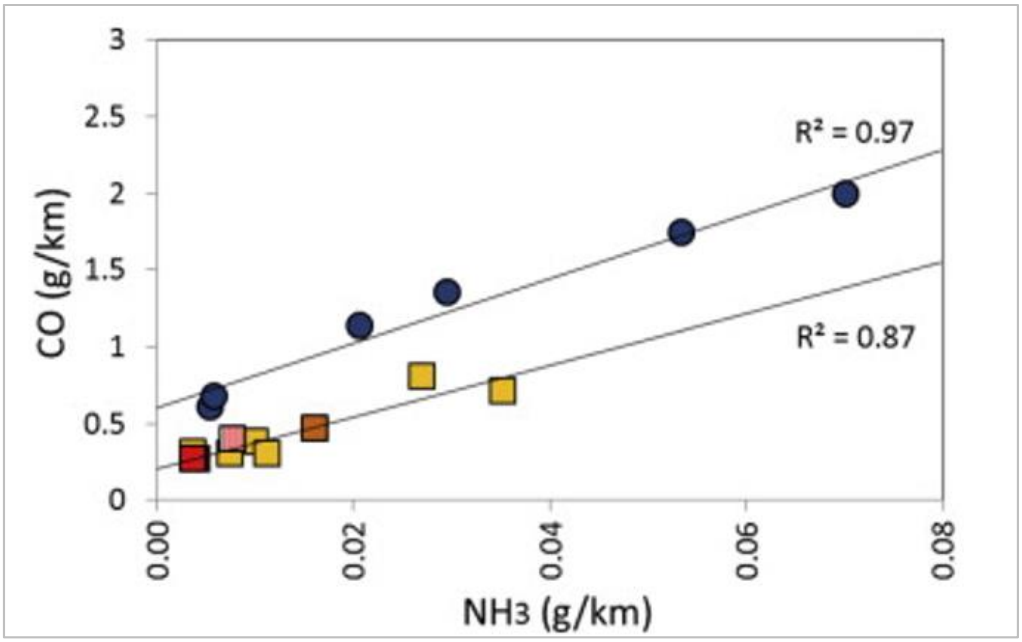

Figure A-3. CO vs. NH_3 emission factors at 22°C (yellow squares) and -7°C (blue circles). Also shown are data from other dynamometer studies performed at 22°C (red and orange squares). From Suarez et al. (2017).

One of the US studies cited (Livingston et al., 2009) reported that the fleet-average NH_3 emission rate based on the Unified Cycle (UC) was 46 mg/km, with the ultra-low emissions vehicle (ULEV)-only average of 27 mg/km. The latter is much higher than the reported ULEV emission rate of 12 mg/km by Suarez-Bertoa (2017) on the Federal Test Procedure (FTP) cycle. According to Livingson et al. (2009):

> *"Although no statistically significant differences were found among different vehicle types, emission standards or driving cycles, the results of this study suggested the highest ammonia emitters are likely to possess the following characteristics: medium-duty vehicles, older emissions technologies, mid-range odometer readings, and higher CO emissions. Aggressive driving cycles were also associated with higher ammonia emission rates."*

Livingston et al. (2009) found that the most aggressive cycle (US06, a certification driving schedule that has higher acceleration and more braking than the FTP) resulted in the highest NH_3 emissions, although the number of vehicles tested was fewer than those tested on the FTP. The UC has been described as more aggressive than the FTP, and similar numbers of vehicles were tested, providing the best evidence for increased NH_3 emissions during more aggressive driving.

A.3.2 Heavy-Duty Diesel Vehicles

Khalek et al. (2015) studied two engines (a 2007 model without SCR and a 2010 model with SCR) run on an engine dynamometer. NH_3 emissions were 0.0025 g/hp-hr for the 2010 engine and undetectable for the 2007 engine. Using the CO_2 measurement of 571.3 g/hp-hr from the same test results and converting this result to fuel consumed of 240 g/kW-hr, the 2010 engine NH_3 emission rate converts to the equivalent of 0.014 g/kg-fuel. This is far lower than the 0.09 g/kg-fuel result from Haugen et al. (2018) for the fleet of heavy-duty diesel vehicles in 2017 of which only 63% used 2010 or later engines.

To provide another reference, Mendoza-Villafuerte et al. (2017) installed a PEMS on a truck with a Euro VI compliant diesel engine, an SCR, and an NH_3 oxidation catalyst. The test was conducted on various road types. Results shown in Table A-1 show a cold start effect, but overall the NH_3 emissions are closer to those of Haugen et al. (2018) versus those of Khalek et al. (2015) especially when considering cold starts. The results for different types of road driving were not significantly different.

Table A-1. Heavy-duty diesel NH_3 emissions reported by Mendoza-Villafuerte et al. (2017).

Road	NH_3 (g/kW-hr)	NH_3 (g/kg-fuel)	Start Condition
Urban	0.0245	0.102	cold
	0.0115	0.048	hot
Rural	0.0270	0.112	cold
	0.0130	0.054	hot
Motorway	0.0315	0.131	cold
	0.0080	0.033	hot

Heavy-duty NH_3 emissions are considerably higher for stoichiometric compressed natural gas (CNG) engines. Thiruvengadam et al. (2016) measured emissions using a trailer-mounted system equivalent to a certification grade laboratory that allows measurements to be taken during on-road driving like a PEMS device. Table A-2 shows results for stoichiometric (spark-ignition) CNG engines compared with a high-pressure direct injection (HPDI) dual-fueled diesel/natural gas compression ignition engine, and a typical modern diesel engine (the latter two with SCR systems). For the Urban Dynamometer Driving Schedule (UDDS), the average NH_3 emission rate for stoichiometric CNG engines was 930 mg/mi (equivalent to 578 mg/km), which is more than 10 times the highest NH_3 emission rates reported for stoichiometric gasoline light-duty vehicles.

A.4 Summary of Mobile Source Ammonia Emission Rates

For gasoline light-duty vehicles, the more robust results are those from the remote sensing study of Bishop (2019) because the number vehicles studied was greater, and the results were similar in magnitude to other remote sensing studies. The Bishop (2019) results also showed that aged vehicles and surface street operation produced substantially higher NH_3 emissions. To facilitate comparisons to other studies, and to rates as modeled in MOVES, we converted the fleet average 0.43 g/kg-fuel (freeway) and 0.62 g/kg-fuel (arterial) emissions rates to mass per distance using the fleet average fuel economy of 22.0 miles/gallon (BTS, 2020) and a typical gasoline fuel density of 6.17 lb/gallon. This results in 55 mg/mi (freeway) and 79 mg/mi (arterial) or 34–49 mg/km. These results are at the high end of the dynamometer and PEMs testing results though nearly identical to the 46 mg/km average found by Livingston et al. (2009). So, the Bishop (2019) results seem the most reasonable

especially given that the greater number of tests conducted included higher emitting aged vehicles in the same fraction as found across the entire fleet.

Table A-2. Heavy-duty NH_3 emissions (mg/mile) reported by Thiruvengadam et al. (2016). ND notes "not detected".

Vehicle	UDDS	Regional	Near Dock	Local	Orange County Transit Authority	Refuse Truck
Stoichiometric CNG Tractor 1	380	570	240	990		
Stoichiometric CNG Tractor 2	820	980	2010	2200		
Stoichiometric CNG Tractor 3	870	910	1790	1480		
Stoichiometric CNG Transit Bus	890				950	
Stoichiometric CNG Refuse Truck	1710					1090
HPDI Dual-Fuel Diesel/Natural Gas Lean Burn Compression-Ignition	89	5	40	20		
2010 Diesel SCR Tractor	ND	ND	ND	ND		
2010 Diesel SCR Refuse Truck	ND					ND

NH_3 emissions for gasoline vehicle cold starts and cold conditions could be higher. Cold starts could add a significant increment of up to 100 mg per cold start based on one Euro VI vehicle test. Cold conditions below freezing (-7°C or 20°F) resulted in a 28–47% increase over those at 22°C based on a few Euro V and VI vehicles.

Aggressive driving could result in a 41% increase in NH_3 emissions according to one study of 34 US vehicles, but the results of Bishop (2019) demonstrated that arterial driving resulted in a similar 44% increase over freeway driving. So perhaps aggressive driving is incorporated in the Bishop (2019) remote sensing results.

Direct light-duty diesel vehicle emissions have been measured at about 8-12 mg/km by Suarez-Bertoa (2017 and 2014). It is unclear if these European emission standard vehicles were designed with the same technology as US heavy-duty diesel vehicles in terms of NH_3 slip control.

The most robust measure of heavy-duty diesel vehicle emissions was the adjusted (to a 100% SCR-equipped fleet) average of 0.14 g/kg-fuel from Haugen et al. (2018) because it was based on a larger fleet of 1844 measurements. To better compare heavy-duty diesel vehicle NH_3 emissions measurements with other results, such as modeled in MOVES, the emissions per energy (kW-hr) or fuel consumed (kg) was converted to emissions per distance. Assuming a typical average fuel economy for larger heavy-duty trucks of about 7 miles/gallon (NHTSA, 2020) and an average fuel density of 3200 g/gallon (EPA, 2009) results in an approximate NH_3 emission rate estimate of 64 mg/mi (40 mg/km).

Table A-3 presents a summary of NH_3 emissions determined from this literature review to be the best estimates available. Original measurements in mass emitted per mass of fuel are also shown as mass emitted per distance using average fuel economy estimates. The MOVES model allows the fuel

economy to be calculated for all conditions, so NH_3 emissions in g/kg-fuel could result in different mg/mi than those shown in Table A-3 when considering different driving conditions.

Diesel vehicles have significant NH_3 emissions only when introduced (via urea injection) for SCR catalysts. To meet emissions standards SCR was installed only in post-2007 light-duty and post-2010 heavy-duty vehicles. Because light-duty gasoline vehicles have had TWC since the 1980 model year and the original measurements were made on the entire fleet, the NH_3 emission estimates shown in Table A-3 are expected to be representative of the entire current gasoline vehicle fleet.

Table A-3. Summary of on-road vehicle NH_3 emission estimates.

Vehicle Type	Model Years[1]	By Fuel Consumption (g/kg-fuel)	By Distance (mg/mi)	Reference
Light-duty gasoline	All TWC (>1980) Highway	0.43	~55	Bishop (2016)
	All TWC (>1980) Arterial	0.62	~79	
Light-duty diesel	<2007	N/A	0	Suarez-Bertoa et al. (2014, 2017)
	>2007	~0.144[2]	16	
Heavy-duty diesel	<2010	0.003	~1	Haugen et al. (2018)
	>2010	0.141	~64	
Heavy-duty CNG	All	N/A	930	Besch et al. (2016)

1 Nearly all <2010 heavy-duty diesel vehicles used 2009 engines without SCR, and <2007 light-duty diesels were not likely SCR so NH_3 would not be introduced into the exhaust stream.
2 Assuming 30% better fuel economy than light-duty gasoline and diesel fuel specifications.

A.5 References

Bishop, G.A., 2019. Three decades of on-road mobile source emissions reductions in South Los Angeles. *Journal of the Air & Waste Management Association*, 69(8), 967–976.

BTS, 2020. Average Fuel Efficiency of U.S. Light Duty Vehicles. Bureau of Transportation Statistics, https://www.bts.gov/content/average-fuel-efficiency-us-light-duty-vehicles.

EPA, 2009. Emission Factors for Locomotives. Environmental Protection Agency (EPA-420-F-09-025, April 2009).

Haugen, M.J., G.A. Bishop, A. Thiruvengadam, D.K. Carder, 2018. Evaluation of Heavy- and Medium-Duty On-Road Vehicle Emissions in California's South Coast Air Basin. *Environ. Sci. Technol.,* 52(22), 13298-13305.

Kean, A.J., D. Littlejohn, G.A. Ban-Weiss, R.A. Harley, T.W. Kirchstetter, M.M. Lunden, 2009. Trends in on-road vehicle emissions of ammonia. *Atmospheric Environment* 43, 1565–1570.

Khalek, I.A., M.G. Blanks, P.M. Merritt, B. Zielinska, 2015. Regulated and unregulated emissions from modern 2010 emissions-compliant heavy-duty on-highway diesel engines. *Journal of the Air & Waste Management Association*, 65(8), 987–1001.

Livingston, C., P. Rieger, A. Winer, 2009. Ammonia emissions from a representative in-use fleet of light and medium-duty vehicles in the California South Coast Air Basin. *Atmospheric Environment*, 43, 3326–3333.

Mendoza-Villafuerte, P., R. Suarez-Bertoa, B. Giechaskiel, F. Riccobono, C. Bulgheroni, C. Astorga, A. Perujo, 2017. NOx, NH3, N2O and PN real driving emissions from a Euro VI heavy-duty vehicle. Impact of regulatory on-road test conditions on emissions. *Science of The Total Environment*, 609, 546-555.

Nevalainen, P., N.M. Kinnunen, A. Kirveslahti, K. Kallinen, T. Maunula, M. Keenan, M. Suvanto, 2018. Formation of NH_3 and N_2O in a modern natural gas three-way catalyst designed for heavy-duty vehicles: the effects of simulated exhaust gas composition and ageing. *Applied Catalysis A: General*, 552, 30-37 (25 February 2018).

NHTSA, 2020. Commercial Medium- and Heavy-Duty Truck Fuel Efficiency Technology Study – Report #1. National Highway Traffic Safety Administration, https://www.nhtsa.gov/sites/nhtsa.dot.gov/files/812146-commercialmdhd-truckfuelefficiencytechstudy-v2.pdf.

Suarez-Bertoa, R., A.A. Zardini, C. Astorga, 2014. Ammonia exhaust emissions from spark ignition vehicles over the New European Driving Cycle. *Atmospheric Environment*, 97, 43-53.

Suarez-Bertoa, R., P. Mendoza-Villafuerte, F. Riccobono, M. Vojtisek, M. Pechout, A. Perujo, C. Astorga, 2017. On-road measurement of NH_3 emissions from gasoline and diesel passenger cars during real world driving conditions. *Atmospheric Environment*, 166, 488-497.

Sun, K., L. Tao, D.J. Miller, D. Pan, L.M. Golston, M.A. Zondlo, R.J. Griffin, H.W. Wallace, Y.J. Leong, M.Y.M. Yang, Y. Zhang, D.L. Mauzerall, T. Zhu, 2016. Vehicle Emissions as an Important Urban Ammonia Source in the United States and China. *Environmental Science Technology*, DOI:10.1021/acs.est.6b02805.

Thiruvengadam, A., M. Besch, D. Carder, A. Oshinuga, R. Pasek, H. Hogo, M. Gautam, 2016. Unregulated greenhouse gas and ammonia emissions from current technology heavy-duty vehicles. *Journal of the Air & Waste Management Association*, 66(11), 1045–1060.

APPENDIX B: SMAT RELATIVE RESPONSE FACTOR DESIGN VALUE SCALING RESULTS

SMAT Output: UDAQ Configuration

Site ID	County	b_pm25_DV	f_pm25_DV
490030003	Box Elder	32.4	33.5
490110004	Davis	28.5	28.3
490353006	Salt Lake	33.4	34.0
490353010	Salt Lake	34.9	35.4
490494001	Utah	31.1	29.8
490495010	Utah	28.4	28.9
490570002	Weber	30.2	30.7

SMAT Output: UDAQ Configuration

Site ID	County	b_crustal	b_EC	b_NH4	b_Ocmb	b_SO4	b_NO3	b_water
490030003	Box Elder	2.0	1.9	2.2	17.2	2.0	5.2	1.5
490110004	Davis	1.3	1.7	3.2	9.2	1.9	8.8	1.9
490353006	Salt Lake	1.6	1.9	3.9	10.3	2.2	10.7	2.4
490353010	Salt Lake	1.4	1.9	3.8	12.6	2.1	10.4	2.3
490494001	Utah	0.7	1.5	4.9	4.6	2.0	14.2	2.8
490495010	Utah	1.9	2.4	3.0	8.8	2.3	7.7	1.9
490570002	Weber	1.1	1.9	3.4	10.1	1.9	9.3	2.0

SMAT Output: UDAQ Configuration

Site ID	County	f_crustal	f_EC	f_NH4	f_Ocmb	f_SO4	f_NO3	f_water
490030003	Box Elder	1.5	1.6	3.4	13.2	2.0	9.4	2.0
490110004	Davis	1.3	1.8	2.9	10.8	1.8	7.6	1.7
490353006	Salt Lake	2.2	1.8	3.6	11.9	2.0	9.8	2.2
490353010	Salt Lake	2.1	1.8	4.0	11.5	2.1	11.0	2.4
490494001	Utah	1.9	2.0	3.4	8.8	2.0	9.2	2.1
490495010	Utah	2.1	2.2	3.1	8.7	2.3	8.0	2.0
490570002	Weber	1.0	1.3	4.3	6.7	1.9	12.5	2.5

SMAT Output: UDAQ Configuration

Site ID	County	rrf_crustal	rrf_ec	rrf_nh4	rrf_oc	rrf_so4	rrf_no3	rrf_water
490030003	Box Elder	0.75	0.85	1.57	0.77	0.99	1.81	1.38
490110004	Davis	0.96	1.08	0.89	1.17	0.96	0.87	0.89
490353006	Salt Lake	1.38	0.97	0.92	1.16	0.90	0.92	0.93
490353010	Salt Lake	1.53	0.96	1.05	0.91	1.02	1.06	1.05
490494001	Utah	2.69	1.26	0.69	1.93	1.02	0.64	0.76
490495010	Utah	1.11	0.94	1.04	0.98	1.01	1.05	1.04
490570002	Weber	0.86	0.70	1.28	0.67	0.98	1.34	1.23

SMAT Output: Ramboll Configuration

Site ID	County	b_pm25_DV	f_pm25_DV
490030003	Box Elder	32.4	33.4
490110004	Davis	28.5	28.6
490353006	Salt Lake	33.4	33.2
490353010	Salt Lake	34.9	35.0
490494001	Utah	31.1	30.6
490495010	Utah	28.4	28.5
490570002	Weber	30.2	30.2

SMAT Output: Ramboll Configuration

Site ID	County	b_crustal	b_EC	b_NH4	b_Ocmb	b_SO4	b_NO3	b_water
490030003	Box Elder	2.0	1.9	2.2	17.3	2.0	5.2	1.5
490110004	Davis	1.3	1.7	3.2	9.3	1.9	8.8	1.9
490353006	Salt Lake	1.6	1.9	3.9	10.3	2.2	10.7	2.4
490353010	Salt Lake	1.4	1.9	3.8	12.7	2.1	10.4	2.3
490494001	Utah	0.7	1.5	4.9	4.6	2.0	14.3	2.8
490495010	Utah	1.9	2.4	3.0	8.9	2.3	7.7	1.9
490570002	Weber	1.1	1.9	3.4	10.1	1.9	9.3	2.0

SMAT Output: Ramboll Configuration

Site ID	County	f_crustal	f_EC	f_NH4	f_Ocmb	f_SO4	f_NO3	f_water
490030003	Box Elder	1.2	1.7	3.9	11.0	2.1	10.7	2.3
490110004	Davis	1.3	1.7	3.3	9.2	1.9	8.9	2.0
490353006	Salt Lake	1.6	1.9	3.9	10.3	2.1	10.7	2.4
490353010	Salt Lake	1.4	1.8	4.2	10.8	2.2	11.8	2.5
490494001	Utah	0.6	1.5	4.8	4.5	1.8	14.2	2.8
490495010	Utah	1.9	2.3	3.2	8.3	2.3	8.2	2.0
490570002	Weber	1.1	1.6	3.5	10.1	1.9	9.6	2.1

SMAT Output: Ramboll Configuration

Site ID	County	rrf_crustal	rrf_ec	rrf_nh4	rrf_oc	rrf_so4	rrf_no3	rrf_water
490030003	Box Elder	0.63	0.90	1.78	0.64	1.07	2.07	1.56
490110004	Davis	1.00	0.99	1.01	0.99	1.01	1.01	1.01
490353006	Salt Lake	1.00	1.01	0.99	0.99	0.95	1.00	1.00
490353010	Salt Lake	1.04	0.97	1.11	0.85	1.03	1.13	1.11
490494001	Utah	0.89	0.99	0.98	0.98	0.89	1.00	0.99
490495010	Utah	1.01	0.97	1.05	0.93	1.03	1.06	1.05
490570002	Weber	1.00	0.85	1.03	0.99	1.00	1.03	1.03